REPUBLIC OF TÜRKİYE

GAZİANTEP UNIVERSITY

GRADUATE SCHOOL OF NATURAL & APPLIED SCIENCES

INVESTIGATION OF WEAR BEHAVIOUR OF GEARS UNDER DIFFERENT WORKING CONDITIONS MANUFACTURED BY 3D PRINTING AND CONVENTIONAL METHODS

M.Sc. THESIS

IN

MECHANICAL ENGINEERING

BY

ABDURRAHMAN GÜNGÖR

JUNE 2023

JUNE 2023

M.Sc. in Mechanical Engineering

ABDURRAHMAN GÜNGÖR

INVESTIGATION OF WEAR BEHAVIOUR OF GEARS UNDER DIFFERENT WORKING CONDITIONS MANUFACTURED BY 3D PRINTING AND CONVENTIONAL METHODS

M.Sc. Thesis

in

Mechanical Engineering

Gaziantep University

Supervisor

Prof. Dr. Necip Fazıl YILMAZ

by

Abdurrahman GÜNGÖR

June 2023

INVESTIGATION OF WEAR BEHAVIOUR OF GEARS UNDER DIFFERENT WORKING CONDITIONS MANUFACTURED BY 3D PRINTING AND CONVENTIONAL METHODS

submitted by **Abdurrahman GÜNGÖR** in partial fulfillment of the requirements for the degree of Master of Science in **Mechanical Engineering, Gaziantep University** is approved by,

Prof. Dr. Mehmet İshak YÜCE
Director of the Graduate School of Natural and Applied Sciences ………..............

Prof. Dr. Mehmet Sait SÖYLEMEZ
Head of the Department ………..............

Prof. Dr. Necip Fazıl YILMAZ
Supervisor, Department of the Mechanical Engineering ………..............

Exam Date: 21/06/2023

Examining Committee Members:

Prof. Dr. Necip Fazıl YILMAZ
Gaziantep University ………..............

Prof. Dr. Ömer EYERCİOĞLU
Gaziantep University ………..............

Prof. Dr. Metin KÖK
Kahramanmaraş Sütçü İmam University ………..............

I hereby declare that all information in this document has been obtained and presented in accordance with academic rules and ethical conduct. I also declare that, as required by these rules and conduct, I have fully cited and referenced all material and results that are not original to this work.

Abdurrahman GÜNGÖR

ABSTRACT

INVESTIGATION OF WEAR BEHAVIOUR OF GEARS UNDER DIFFERENT WORKING CONDITIONS MANUFACTURED BY 3D PRINTING AND CONVENTIONAL METHODS

GÜNGÖR, Abdurrahman
M.Sc. in Mechanical Engineering
Supervisor: Prof. Dr. Necip Fazıl YILMAZ
June 2023
82 pages

The main purpose of this research is to examine the wear behavior of thermoplastic gears produced by machining and additive manufacturing under different operating conditions. In this study, PA6 (Polyamide) plastic gear produced by machining method and Ultem 1010 gear produced by additive manufacturing method were used. These gears were tested for wear behavior at different cycles against the steel gear (1040 steel). These gears (Ultem 1010&PA6) were operated at 400 rpm, 800 rpm and 1200 rpm and completed 1 million revolutions. Temperature, noise, torque and surface roughness were measured during wear tests. The primary purpose of these tests is to reveal the wear differences of PA6 and Ultem 1010 gears. Ultem 1010 gear produced by additive manufacturing is an engineering thermoplastic with good mechanical properties and heat. When the temperature, wear, noise and torque results were examined, it was concluded that the PA6 gear performed better at low and medium speeds, while the Ultem 1010 gear performed better at high speeds.

Key Words: Additive Manufacturing, Wear of plastic gears, Ultem 1010, PA6

ÖZET

3B BASKI VE GELENEKSEL YÖNTEMLERLE ÜRETİLEN DİŞLERİNİN FARKLI ÇALIŞMA KOŞULLARI ALTINDAKİ AŞINMA DAVRANIŞLARININ İNCELENMESİ

GÜNGÖR, Abdurrahman
Yüksek Lisans Tezi, Makine Mühendisliği Bölümü
Danışman: Prof. Dr. Necip Fazıl YILMAZ
Haziran 2023
82 sayfa

Bu araştırmanın temel amacı, talaşlı imalat ve eklemeli imalat ile üretilen termoplastik dişlilerin farklı çalışma koşullarında aşınma davranışlarının incelenmesidir. Bu çalışmada talaşlı imalat yöntemi ile üretilen PA6 (Polyamid) plastik dişli ve eklemeli imalat yöntemi ile üretilen Ultem 1010 dişli kullanılmıştır. Bu dişliler, çelik dişliye (1040 çelik) karşı farklı döngülerde aşınma davranışı açısından test edilmiştir. Bu dişliler (Ultem 1010&PA6) 400 rpm, 800 rpm ve 1200 rpm'de çalıştırılarak 1 milyon devir tamamlamıştır. Aşınma testleri sırasında sıcaklık, gürültü, tork ve yüzey pürüzlülüğü ölçülmüştür. Bu testlerin öncelikli amacı PA6 ve Ultem 1010 dişlilerinin aşınma farklılıklarını ortaya çıkarmaktır. Eklemeli imalatla üretilen Ultem 1010 dişlisi, iyi mekanik özelliklere ve ısıya sahip bir mühendislik termoplastiktir. Sıcaklık, aşınma, gürültü ve tork sonuçları incelendiğinde PA6 dişlisi düşük ve orta hızlarda, Ultem 1010 dişlisinin ise yüksek hızlarda daha iyi performans gösterdiği sonucuna ulaşılmıştır.

Anahtar Kelimeler: Eklemeli İmalat, Plastik dişlilerin aşınması, Ultem 1010, PA6.

''Dedicated to my family''

ACKNOWLEDGEMENTS

First of all, Prof. Dr. Necip Fazıl YILMAZ thank you very much to my teacher. I would like to express my deepest respect and sincere thanks to. I will always be grateful for their valuable advice, insight, oversight and encouragement during this research.

I would like to thank lecturer Musa YILMAZ and Res. Asst. M. Furkan KALKAN for always sharing their support and knowledge within the scope of the thesis.

I would like to express my endless thanks to my beloved mother and father who always supported and believed in me and supported my education and training life.

I would like to thank my dear friend and source of motivation, Şule Güngör for her support throughout my thesis work.

I would like to express my endless thanks to my dear friend Gülşah ANGIN, who was with me during the thesis process, whom I loved very much, who believed and trusted me during this process.

I would like to thank Research Assistant M. Ali AKELOĞLU, Research Asistant A. Emin KARADAĞ and lecturer Engin TEK for their help and knowledge in the experimental processes.

I would also like to thank the Mechanical Engineering Department Workshop and Laboratory staff for their assistance.

TABLE OF CONTENTS

Page

LIST OF TABLES

LIST OF FIGURES

Page

LIST OF SYMBOLS/ABBREVIATIONS

μ	Coefficient Of Friction
F	Force
N	Newton
g	Gram
CoF	Coefficient Of Friction
AM	Additive Manufacturing
CM	Conventional Manufacturing
CAD	Computer Aided Design
3D	Three Dimensional
RPM	Revolutions Per Minute
FDM	Fused Deposition Modeling
T_g	Glass Transition Temperature
ASA	Acrylonitrile Styrene Acrylate
PC	Polycarbonate
ABS	Acrylonitrile Butadiene Styrene
PEEK	Polyether Ether Ketone
PLA	Polylactic Acid
SEM	Scanning Electron Microscopy

CHAPTER 1
INTRODUCTION

1.1 Introduction

Gear systems, which are widely used in today's technology, are power and motion transmission elements used in almost every machine. Important issues in gear manufacturing are sufficient strength, lightness, economy, quiet operation, easy manufacturability etc. can be listed as. In order to prevent losses by using energy and materials economically, ideal working conditions must be found first.

Metals especially AISI 8620 and 1040 and cast iron as well as copper, zinc, aluminum alloys are used as materials in gear wheels, whose uses are very common. Plastic materials, which have become increasingly widely used recently, are preferred over metal gears in gear systems. These plastics can be counted as polyamide (nylon), acetal (derlin), cast polyamide, kestamide, teflon, fiber etc. With the use of these materials, features such as silent operation, oil-free operation, light weight, suitability for mass production, damping of impacts and vibrations, and production economy are provided in gear systems. Their disadvantages are their low load carrying capacity, low thermal conductivity, and inability to determine their lifetime. Studies on this subject are increasing day by day. In addition to these, glass reinforced, and lubricating thermoplastics have lately been employed as gear materials. Glass makes up 30% of the weight of these technical polymers and a lubricant of 15% is applied. These lubricants include polycarbonate, polysulfon, acetal, polypropylene, nylon, polyurethane, and polyester, among others. Furthermore, composite-material gears have a higher load carrying capacity, reduced thermal expansion, greater durability, and fatigue strength.

The purpose of the tests is to show how traditional and additive manufacturing methods affect gear wear. The investigations used the PA6 gear made by machining and the ULTEM 1010 gear made by additive manufacturing. Hobbing machines are commonly used to make gears that can be made with cutting dies, extrusion, and sintering. New ways for producing high-quality gears will overcome the constraints of old technologies and provide alternatives. Recently, 3d printing technology has proven to be a viable method of manufacture, and it has begun to gain traction in the manufacturing industry as technology has advanced.

Plastic gears are generally manufactured by injection molding. However, traditional methods have disadvantages in terms of time and cost. The main focus of additive manufacturing technology is that the desired part can be manufactured directly with a computer aided design system. This technology is quite different from traditional methods, and it prevents material waste during production (Tezel et al., 2020). Plastic is made from organic materials. It is derived from natural resources such as plastic, cellulose, coal, natural gas, salt and crude oil. Crude oil is a complex mixture of thousands of different components. Due to the complex mixing, plastic materials of various structures and qualities can be made. It must be processed to be useful. As polymer mixtures, plastics consist of two or more polymers in homogeneous or heterogeneous structure.

Plastics are divided into 4 main headings; Thermoplastic, Elastomer, Thermoset and Compounds.Plastic gears can be produced in different structures and features. Polyethylene (PE), Polyvinylchloride (PVC), Polypropylene (PP), ABS (acrylonitrile butadiene-styrene),Polystyrene (PS),Nylon, Polycarbonate (PC), Polytetrafluorethylene (Teflon) and Epoxies are just a few examples. Due to its high strength, hardness, impact and oil resistance, chemical resistance, abrasion resistance and self-lubrication, especially hardness, heat resistance and ease of availability, PA6 plastic gear with semi-crystalline structure has been used. Due to its low cost, it is widely used in various industries, including industry, clothing, decoration and technical plastics

Another gear used in this investigation is ultem 1010, additively manufactured gear. Ultem (Polyetherimide-PEI) is a high-performance engineering thermoplastic with excellent heat, flame, and chemical resistance. It is also flame retardant and can be used in high-performance applications. Ultem 1010 is a great FDM printing material for advanced tooling and prototyping applications in areas such as automotive, aerospace, gear manufacturing, medical, and food production due to its strong properties. Ultem 1010 is selected since it has one of the best additive manufacturing resistances. The transparency of PEI resin is yellow. Ultem's weather resistance and ability to withstand UV rays is a standout characteristic (Han et al., 2019a)-(Y. Zhang et al., 2020).

In this study, two gears with the same gear features and different feature structures were used, ULTEM 1010 and PA6. Unlike previous research, multiple analyses of these two gears were carried out experimentally and in different cycles. Both gears exhibited wear behavior against the steel gear in tests. The purpose of the tests is to show that Ultem 1010 gear outperforms the traditionally manufactured PA6 gear in terms of wear performance. Expectations were reached based on the findings of the experiments.

1.2 Organisation of The Thesis

This thesis study is divided into seven chapters and general information about each chapter is given below.

In the first chapter, general information about the gears, the general properties of the plastic gears used and their use in the industry, as well as the plastics are given.

In Chapter 2, summaries of the studies and researches available in the literature on the wear, friction and thermal behavior of plastic and steel gears are given.

In Chapter 3, additive manufacturing will be briefly mentioned. In addition, brief information will be given about the types of additive manufacturing and the materials used in this method.

In Chapter 4, detailed explanations about wear and its theory are given. What are the main wear types and their effects are explained in detail.

Chapter 5 provides information on the material method. Information about the experimental parameters and equipment used in the experiments, measuring instruments, wear test equipment, general characteristics of the gears used and their production are presented.

Chapter 6 contains conclusions and discussions. The research results are shown with graphics and figures. As a result of the tests performed on the gears used, the results such as the amount of wear, temperature, wear, torque and noise relations are explained graphically.

Chapter 7 provides information on the conclusions and implications.

CHAPTER 2
LITERATURE SURVEY

2.1 Introduction

In this section, a brief summary of the studies in the literature is presented. Many studies have been carried out on wear, thermal behavior and surface roughness of thermoplastic gears. In this section, studies in the literature on the PEI gear produced by 3D printing and the PA6 gear produced by machining are explained.

2.2 Literature on Wear in Plastic Gears

Ye Zhang et al.(Y. Zhang et al., 2020) they compared 5 different gears produced with a 3D printer with the Nylon 66 gear, which is widely used in the industry, based on factors such as wear, friction, thermal behavior. Gears produced by 3D printing are Nylon 618, Nylon 645, Alloy 910, Markforged Nylon and Onyx gears. Nylon 66 gear was produced by injection molding. Abrasion tester was used in the study. Tests were carried out at room conditions at different cycles and torques. Nylon 618 and Onyx gears showed more stable structure under 10 Nm. Nylon 618 gear showed better thermal performance compared to gears produced with other 3D printers due to better wear, friction and crystal structure. Nylon 618 performed better at low, and medium torques.

S. Satheesh Kumar et al. (Sathees Kumar et al., 2021) they worked on how to reduce the temperature resulting from working in polyamide gears. They found that overheating occurred in the root part of the polyamide gears as a result of the temperature, and as a result, they saw that serious wear and durability decreased. As a solution to this, they drilled holes in the pitch circle diameter of the tooth. Theoretically, experimental studies were carried out on ANSYS, and they carried out the experiment on the parogram at different torques of 300 and 500 Nm. As a result, it was seen in the simulation that the tooth does not heat up due to the openings, and it expels of the hot air conventionally, which they concluded that increases the life and durability of the tooth.

Ken Mao et al. (Mao et al., 2019) they compared POM and 28% glass fiber reinforced GFR POM gears. Aluminum molds were designed for both gears, gear pairs were produced by injection molding method. Special gear equipment was designed for this study. For gears operating at 2000 rpm, the transition torque for the POM gear was 7.5 Nm, for the GFR POM 11 Nm. The wear on the gears has been too much since these torque values. They found that GFR POM was more durable.

Tunalioglu et al. (Tunalioglu & Torun, 2021) they produced PLA spur gears with FDM technology and exposed them to wear. This gear worked with the st37-2 gear in different cycles and torques. Their purpose is to investigate the specific wear amount by increasing or decreasing the torque and rotational speed and keeping it constant. Gear pairs worked 10× 104 cycles at 0.5 ,1,1.5 Nm at 300,600,900 rpm. As a result of the tests, they obtained that the specific wear amount of the plastic gears increases with the increase of the load (torque), and the specific wear of the gears decreases with the increase of the torque by keeping the torque constant. They found that the contact time of a single tooth increased with the decrease of rotational speed at constant rotational speed, and as a result, the strain rate decreased. In the results of the experiment, they found that the increase in the strain rate of the polymer materials increases the hardness and strength, which increases the wear resistance of the material.

Srecko Glodez et al. (Polanec Brigita et al., 2021) they investigated the wear behavior of the coated POM gear at different torques. Al, Cr and CrN coatings are applied to the POM gear. Since the coatings made were less than 500 nm, it did not have a significant effect on the wear resistance. Torque was applied at 16, 20, 24 and 30 Nm and worked at 1000 rpm. As a result of the tests and experiments, it was seen that the CrN coating reduces the wear more, and then the Cr coating follows.

Shivdayal Patel et al. (Raghav et al., 2022) they conducted research on the stresses formed in the tooth roots and the resulting cracks. They advanced experimentally and theoretically. They determined the backup ratio in the teeth as 0.8 and 1.5 and obtained positive results as a result of experimental studies of the gears in long cycles. They also found that when they increased the crack angle from 180° to 225°, the fatigue life was significantly reduced for both static and dynamic loading.

Prashant Kumar Singh et al. (Singh et al., 2018) they investigated the thermal and wear performance of 3 different thermoplastic gears. The gears used in the study are ABS, HDPE and POM, and these gears were obtained by injection molding. They did the tests at different torque and rotational speeds. These torques are determined as 0.8, 1.2, 1.6 and 2 Nm rotation speeds 600, 800, 1000 and 1200 rpm. In the tests made, ABS teeth failed at 2 Nm 30,000 cycles due to excessive wear on, HDPE gear failed at 1.1 million cycles at 2 Nm due to cracks in the 1.1 tooth roots, and POM gear failed at any torque value. It has completed 2 million cycles. In the test results, they found that the maximum increase in surface temperature was maximum for POM and minimum for HDPE. The specific wear rate in polymer gears increases with increasing load, ie torque, but decreases with decreasing rotational speed.

Hüseyin Imrek (Imrek, 2009) has worked to reduce overheating in nylon gears and to increase the life of this gear. Nylon 6 gear overheats and breaks in tooth roots, cracks, excessive softening and this causes damage. Solved this issue via gear modification. He used 3 different gears in his work. The gears used are modified nylon 6, unmodified nylon 6 and AISI 1045 steel alloy gear. Gear modification is an applied change in the width of the tooth. For this reason, he saw that the tooth had no effect on the tooth contact ratio and slip speed between gears. The tests carried out in his study are 1000 rpm rotation speed and 3 different torque values. He observed that the modified nylon 6 gear showed lower tooth temperature as a result of the tests, which caused a decrease in the wear rate compared to the unmodified gear.

K. Mao et al. (Mao et al., 2010) In this study, both experimental and numerical studies were carried out on the thermal and wear performance of acetal gears when they reach the critical loading value. They used a gear wear device for the tests. Gear model has been created for experimental studies on gear surface temperature change. Experiment steps; They were at 500, 1000 and 1500 rpm and worked at torque values between 7-16 Nm. They found that acetal & acetal gear pairs had more wear after 1000 rpm and 9.5 Nm, and this value was the critical loading point. After this point, they saw that the gear teeth also melted, causing thermal failure.

Adis J. Muminovic et al. (Muminovic et al., 2022) investigated the effect of filler percentage on nylon gears in additive manufacturing. They determined the filling percentages as 20-40-60-80 and 100 %. Parameters such as filling type, shell thickness and production rate are fixed for the produced gears. Gear wear device was designed for this study. The starting torque of the teeth with 20% and 40% filling percentage was determined as 2.4 Nm and 1200 rpm rotation speed. In the 20% filling percentage, the torque increased to 2.5 Nm at 5800 rpm and then a sudden decrease was experienced. The main fault here is the transmission of the fault from the gear teeth to the gear body. With 40% filling percentage, surface measurements are taken in the gear every 2500 seconds and the gear has reached a torque of 6.2 Nm in 76550 seconds. After this point, the gear has failed. They set the starting torque as 9 Nm in 60-80% and 100% filled teeth and 1840 cycles worked in 60% filled gears and failed at 10.5 Nm. In gear with 80% filling, tooth damage occurred as a result of the increase in bending stress after 2250 rpm at 13 Nm. Finally, they found that the 100% filled tooth provides slightly longer service life than other gears. It worked 5 minutes longer than the 60% and 80% filled teeth. However, in this gear, a malfunction occurred as a result of intense wear and melting on the tooth surface, at 10.3 Nm 7650 cycles.

Tugce Tezel et al. (Tezel et al., 2020) Steel gears produced by additive manufacturing (DMLS St-420) and steel gears obtained by traditional method (Hobbing machine) were compared according to the wear loss, efficiency, damage and surface analysis results as a result of the tests. They produced 2 polished and unpolished gears by additive manufacturing. Here, efficiency and wear loss were the points they paid the most attention to. The tests were carried out at 250, 500 and 1000 rpm at the parameters 0.25 and 0.5 Nm and worked for 10^5 cycles. As a result of tests and analysis, they found that gears produced by additive manufacturing had a higher structure in terms of density and hardness. In particular, the gear with the polished surface provided better performance in terms of hardness. As a result of the tests, the highest Fe loss was seen in the DMLS420 Unpolished gear. They concluded that additive manufacturing gears are better than conventional gears and can be replaced.

Duzcukoglu et al. (Düzcükoglu Hayrettin, 2010) they worked on reducing the thermal and wear behavior of polyamide gears. They used three PA6 and AISI 8620 gears in their work. PA6 gear is made of cast polyamide and produced by hobbing machine and also carbonized AISI 8620 steel gear. The teeth of one of the 3 PA6 gears used are in standard form, without any treatment. They drilled holes in the other 2 polyamide gear teeth and tooth body and revealed 2 different configurations. Their aim is to minimize the heat accumulated in the tooth and on the tooth surface and reduce the amount of damage. Experiment stages applied 6.1, 10.3 and 18.1 N/mm torque and applied 1000 rpm as $6.48*10^5$ cycle. First type gear configuration, holes were drilled in the teeth, as a result of the tests, they saw that the temperature decreased on the tooth surface, but the heat accumulated in the pitch part of the standard PA6 gear more damage was observed.

In the second type gear configuration, in addition, the holes drilled into the tooth bodies saw that a significant amount of heat was removed from the tooth body. In the second type gear configuration, they found that the onset of thermal damage in the pitch region as a result of the increase in the load applied to the tooth at 18.1 N/mm. They found that the surface temperature was the result of radial holes drilled in the second type of gear configuration.

K. Mao et al.(Breedsa et al., 1993) they thought that there are few studies on the wear behavior of polymer gears in the literature. More studies were conducted on metal and steel gears. They used acetal and nylon gear pairs in their studies. Gears at 500 and 1000 rpm under different torques of 5 Nm, 10 Nm, 15 Nm and 20 Nm, measurements were taken every 10 minutes and they worked for 2 million cycles. For these tests, a wear test device was designed, and a torque arm and weight were used to obtain different torques. Wear/deflection characteristics were measured throughout the tests.

As a result of the tests performed, fractures occurred in the tooth roots near the pitch part of all nylon gears, it did not change the result of high or low speed. However, this situation, tooth breakage, was not seen in acetal gears. To obtain the wear amount, the weights taken before and after the test were obtained. Although the wear of the acetal gear was less than the nylon gear, it showed a large viscoelastic deviation.

K. Mohan Harsha et al. (Harsha et al., 2021) they investigated the potential of three different thermoplastic materials used in plastic gear applications such as ABS, PLA and Nylon. The gears used in the study were produced by 3D printing. FDM technology is used in gear production.

Gear assembly has been designed for the tests to be carried out. Gears worked at 600 rpm, 800 rpm and 1100 rpm and under a torque of 1,364- 1,388 Nm, and each gear worked an average of 1.2 million cycles. As a result of the tests made; It has been concluded that the wear rate for the polymer gear increases with the increase in rotation speed, and the ABS gear has the maximum specific wear rate in terms of wear, and the Nylon gear has the minimum specific wear rate.

K. Mao et al. (Mao et al., 2009) conducted extensive studies of the friction and wear behavior of polymer gears (acetal and nylon). Gears produced by injection molding are primarily; They worked as acetal against acetal gear and as a nylon gear against a nylon gear, and then changed them as a drive and driven gear between acetal and nylon gears. For Acetal & Acetal gear pairs at 1000 rpm, a torque of 7-16.1 Nm was studied, and it was observed that the wear increased when the torque increased. The first 2 stages of wear up to 9 Nm have been observed. At torques above 10 Nm, the teeth broke due to thermal bending in the acetal gears and the tooth thickness of the teeth melted about 40%. Nylon & nylon gear pairs were operated at 1000 rpm and torque range of 5 -20 Nm. At torque values above 10 Nm, 3 steps of wear were observed. In the nylon&nylon gear pair, tooth breakage occurred in the gear with the driver.

2.3 Place of this Work in the Literature

The above discussion shows the difference between the gears produced by 3D printing, instead of the polymer gears produced in the traditional way, which is widely used in the industrial sector, and an alternative 3D printed gear.

The aim of this study is to examine the wear behavior of the Ultem 1010 gear produced by 3D printing and the PA6 gear produced by machining under different operating conditions. A wear test device was made for the tests to be carried out and the parameters were determined based on the literature.

It has been observed that gears produced with 3D printing give better results.

CHAPTER 3
ADDITIVE MANUFACTURING

3.1 Introduction

In this section, general information about additive manufacturing and brief information about its types will be given. Fused deposition modeling (FDM) will be mentioned in detail. Because the produced PEI gear is obtained with FDM technology.

3.2 Additive Manufacturing

Conventional manufacturing methods commonly used in the industry can be generalized as turning, milling, drilling, shaping, grinding, etc. as machining methods, and casting, plastic forming and welding as chipless manufacturing methods. Apart from these, unconventional advanced manufacturing methods such as electroerosion, laser, ultrasonic, pressurized water jet and plasma processing are also used. One of the rapidly developing manufacturing methods that has entered the manufacturing sector in recent years is additive manufacturing technologies (Wong & Hernandez, 2012).

According to the ASTM standard, additive manufacturing (additive manufacturing, additive manufacturing, 3D printing) is the process of combining materials, often layered on top of each other, to make objects from 3D model data, as opposed to subtractive manufacturing methodologies such as traditional machining (Monzón et al., 2015) .In other words, it is the process of combining materials layer by layer in order to produce various objects from 3D model data, and it is the opposite of production methods (machining) based on the principle of removing the material by processing. In recent years, it is seen that additive manufacturing methods are widely used in the field of manufacturing technologies compared to classical methods. With additive manufacturing, it is possible to manufacture models, prototypes or final products (Wong & Hernandez, 2012).

Aircraft, automobiles, spare parts, bicycles, toys, robots, sculptures, accessories, hand tools, chairs, armchairs, glasses, medical equipment, chemicals, pharmaceuticals, dentistry and medicine sectors, aerospace, even weapons. In addition to various products, three-dimensional printers that can even produce artificial organs designed to be transplanted into the human body have actually been developed and used since the 1980s. Small and improved desktop models of this technology, which has been used in the industrial sector for a while, are now also used in homes (Yao et al., 2016).

Additive manufacturing technologies provide many benefits. This technique eliminates the need for the necessary tools, labor, and machines when producing using conventional techniques. Eliminates serious labor-intensive operations (milling, turning, post-production chip clearing, etc.). Provides greater design freedom versus conventional casting and machining. Prototypes of the designs made faster than traditional methods can be produced and can be examined. Short production cycle time: complex parts can be produced in layers in a few hours on additive machines. Total cycle time, including post-processing, is usually a few days or weeks and is often much shorter than conventional metallurgical processes, which often require production times of several months.

3.3 Additive Manufacturing Production Process

First of all, the CAD model of the part to be produced by the additive manufacturing method is created. This CAD model is converted to stl file format. Almost all additive manufacturing technologies use the STL file format. The term STL comes from 3D Systems' STereoLithography, the first commercial additive manufacturing technology used in the 1990s. STL is a CAD model geometric as a de facto standard.

It's a simple way of describing it. Any design data, design history etc. deleting it divides the surfaces of the model into triangular surfaces. The minimum dimensions of these triangles can be set in any CAD software. In short, additive manufacturing technology is the transformation of a 3D CAD model into a triangular lattice surface model (STL) and sliced into layers with special software, then using a 3D printer to start the product layer by layer, starting from the base by the creation process. The additive manufacturing process of a gear is shown in Figure 3.1.

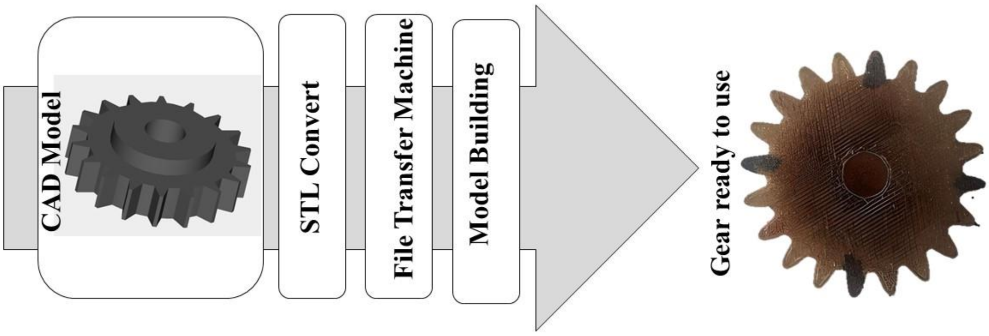

Figure 3.1 Additive manufacturing processes

3.4 Materials Used in Additive Manufacturing

It is possible to use many different materials to create 3D printed objects. With AM technology, jet engine parts can be manufactured from advanced metal alloys, aircraft industry, aerospace, medical devices can be made and parts can be created up to foodstuffs. There is an additive manufacturing method for many material groups. Some material groups shown in Figure 3.2;

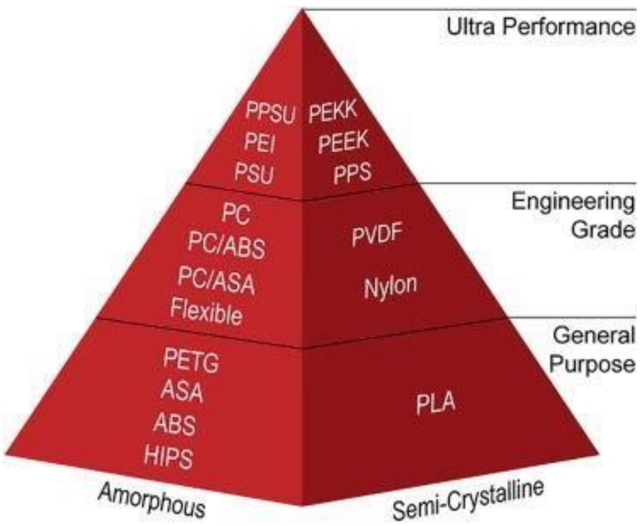

Figure 3.2 Material groups

3.4.1 ABS

ABS (Acrylonitrile Butadine Styrene) (Figure 3.3) is a light but rigid thermoplastic polymer that isalso used quite frequently in the plastic injection industry. ABS, a petroleum product,can be dissolved with acetone. Printer products produced using ABS can be used between -20°C and 80°C. In addition to being a tough and rigid material, ABS plastic is preferred because it has high impact resistance, can be processed easily, is easy to manufacture, can be painted, and is a light material (Olivera et al., 2016).

Figure 3.3 ABS filament

3.4.2 PLA

PLA (Polylactic Acid) is an organic biopolymer and thermoplastic produced from corn starch and sugar cane (Figure 3.4). Therefore, it is not harmful to human health. Compared to ABS,it has a brighter appearance. A 3D Printer using FDM technology can print PLA. Except 3D printer; It is also found in some packaging materials, cling films, plastic containers and plastic water bottles. Basic features (Roy & Mukhopadhyay, 2020; Valino et al., 2019);

- The printing temperature is usually between 190°C – 220°C.
- Bed temperature is recommended between 50°C – 70°C.
- No lifting and cracking problems during cooling.
- It is quite easy to print compared to ABS.

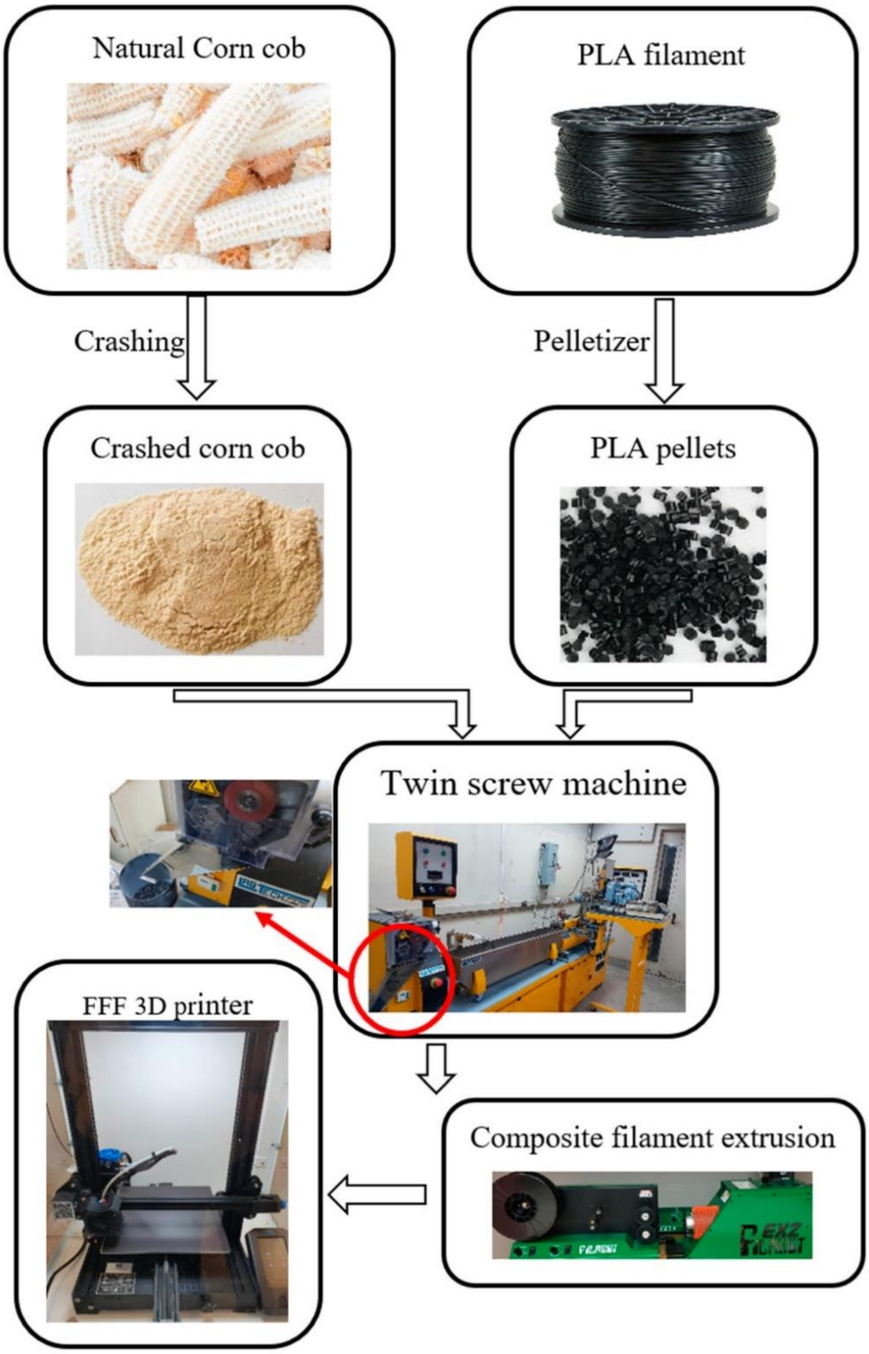

Figure 3.4 PLA filament(Fouly et al., 2022)

3.4.3 PC

PC (Polycarbonate) is a strong type of material used in industry. Durable and transparent materials such as helmets and safety glasses are produced from polycarbonate. PC is suitable for use in 3D printers as it is a thermoplastic.

PC material is a type of high temperature resistant material that can stretch to a certain extent. Parts printed from PC material in 3D printers can maintain their hardness and shape up to 120°C. The bond strength between layers is higher than other filament types.

The optimum conditions for PC filament are provided by 3D printers with a completely closed printing area and an indoor temperature between 45°C-90°C. The higher the indoor temperature, the higher the print quality and durability will be (Kaur & Pavia, 2020; Reich et al., 2019).

3.4.4 PEI

Polyetherimide or PEI material is an amorphous thermoplastic with high mechanical strength and rigidity. PEI polymer is drawn into sheet and rod shapes using resin. Unfilled PEI thermoplastic is transparent and yellow in color and has outstanding mechanical, thermal and electrical properties. In the filled grades, the addition of glass fiber reinforcement (Figure 3.5) along with extrusion techniques results in a polyetherimide with higher tensile strength and stiffness as well as improving dimensional stability.

Polyetherimide has extremely high creep resistance and high continuous operating temperature over a wide temperature range. Moreover, very good hydrolysis resistance combined with dimensional stability complements the polyetherimide properties (Yilmaz et al., 2022),
(Han et al., 2019b).

Figure 3.5 Glass fiber reinforced

3.5 Additive Manufacturing Types

Production types, devices, working methods of devices, materials used, manufactured parts and qualifications that are widely used in today's additive manufacturing technology are included. In this section, some types of additive manufacturing will be discussed. But FDM will be mentioned in a little more detail.

3.5.1 SLA

SLA (Stereo Lithography) is the oldest 3D printing technology, first invented by Chuck Hull in 1983. SLA works on the basis of curing the resin by exposing a layer of a photosensitive liquid resin to a UV laser beam. Scanning stereolithography processes shown in Figure 3.6.

In this method, which is the first rapid prototyping process, the process starts with the photopolymer liquid resin being filled into a tank and a moving platform placed just below the liquid resin surface. With the computer-controlled scanning system, the sections corresponding to the previously sliced sections on the liquid resin surface are solidified with the UV laser. When the layer is complete, the platform layer pulled down to the thickness (Phillips et al., 2020), (Scott et al., 2012).

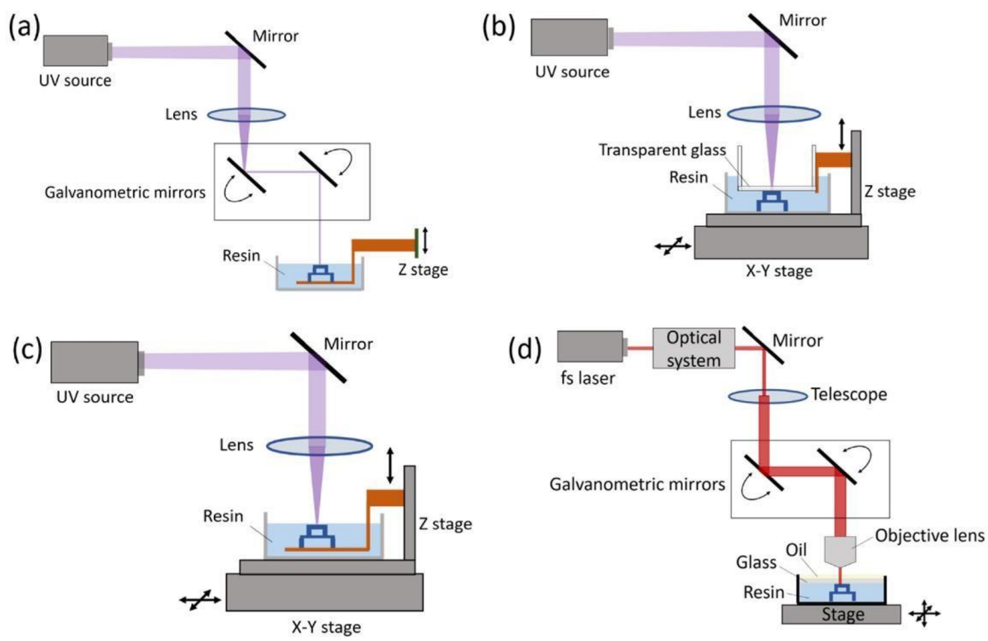

Figure 3.6 Scanning stereolithography processes. (a) Dynamic light beam scanning for stereolithography. (b) The system of constraint surfaces. (c) The free surface system. (d) A typical apparatus for two-photon polymerization (2PP) (Huang et al., 2020) .

The layer thickness varies between 0.025 and 0.5 mm. A new layer of liquid photopolymer is coated on the resulting empty volume. The next layer is completed by building on the previous layer. Thanks to the stickiness of the material, the layers stick together. During the construction, supports are built to the empty parts under the part to prevent the part from moving. Post-process support they leave the piece (Chockalingam et al., 2006; Z. chen Zhang et al., 2019).

With SLA technology, flexible, durable, clear products with high impact resistance can be obtained. However, when photopolymer materials are exposed to UV light for a long time, the materials may crack or break as a result of embrittlement. By means of this method, smooth surfaces can be formed by giving a very precise shape (Manapat et al., 2017; Pagac et al., 2021).

Photopolymer materials are not very stable and their mechanical properties are variable. Since the treated area is filled with liquid resin, only one material can be used at a time in SLA technology. In this method, detailed surfaces are created where the separation of the layers is not felt due to the low layer thicknesses. Unlike other methods, due to the removal of the object from the liquid, protruding forms, reverse angles, and separate parts are produced while supporting structures are added to the print to be cleaned later. Although high resolution outputs are obtained, the robustness of the outputs in stereolithography is compared to other methods stays low (Roy & Mukhopadhyay, 2020),(Szykiedans & Credo, 2016; Z. chen Zhang et al., 2019).

3.5.2 FDM

It is a system based on the principle that the layer formed by melting fibrous thermoplastic materials is suddenly cooled and adhered to the previous layer. In this process, a plastic or wax material is extruded through a nozzle that follows the cross-sectional geometry of the part. The model material is in the form of a thin plastic filament. Sometimes it also uses plastic granules fed from the chamber instead of filament (Gordelier et al., 2019).

The nozzle contains a heating element to keep the thermoplastic at a temperature just above its melting point so that the plastic flows easily over the nozzle and forms a layer (Figure 3.7). After flowing through the plastic nozzle, it suddenly hardens and adheres to the layer below. After the construction of one layer is completed, the platform descends and the extrusion nozzle builds the other layer. Layer thickness and vertical dimensional accuracy depend on the diameter of the extrusion nozzle. This diameter ranges from 0.178 mm to 0.356 mm. A resolution of 0.025 mm can be achieved in theXY plane (Chaudhari et al., 2018).

This method is generally preferred in rapid prototyping and few mass production situations. With this technique, it is possible to manufacture multi-part, movable mechanisms and complex parts. ABS, PLA, polyamide, polycarbonate, polyethylene, polypropylene and investment casting wax can be used as model material. In this method, support material is used while producing the model and a second nozzle has been added to the system in order to use a different support material.

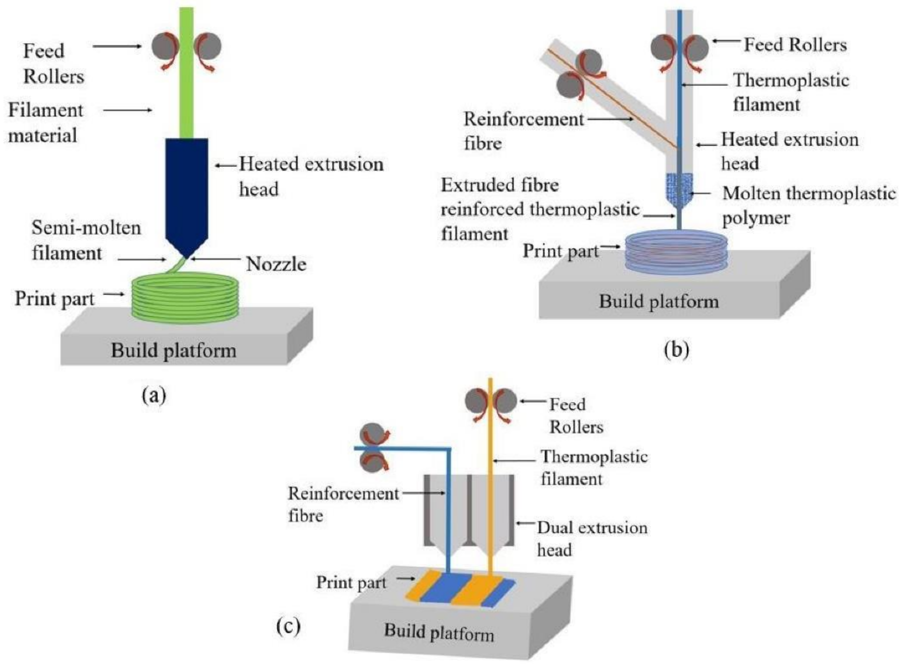

Figure 3.7 Typical FDM printer for short fiber-reinforced composites and polymers (SFRC). (b) Continuous fiber-reinforced composites printed using a co-extrusion FDM printer (CFRC). (c) CFRC dual-extrusion FDM printer (Wickramasinghe et al., 2020).

Process steps:

- Solid material in the form of wire called filament is directed to the heater head withthe help of reel and motor.
- The solid material reaching the head is heated and becomes semi-fluid.
- The semi-fluid material flows from the head on a specific path predetermined by thesoftware. As soon as the semi-fluid material leaves the head, it cools and solidifies andone of the layers forming the model geometry is thus completed.
- This layer, which is completed by solidifying, forms the basis for the new layer to beknitted as a result of one unit (as much as layer thickness) movement of the head or production table.
- This process continues until all the layers that make up the model are formed.
- The support structures in the completed model are cleaned from the physical model by breaking them or (if the 3D printer supports it) by dissolving them in water, and thepart becomes ready for use.

3.5.3 LOM

The main components of the system are a feed mechanism that propels the sheet on the platform, a heated roller to bond the sheet to the substrate with pressure and heat, and a laser that cuts the contour of the part at each layer. The piece is affixed to the previous layer of the laser cut adhesive coated thin sheet is produced with. A laser cuts the contour of the part at each layer. After each cutting operation is completed, the platform descends as much as 0.05-0.5 mm, as the thickness of the thin plate, and another thin plate is advanced onto the previous layer with the help of the feeding mechanism (Parandoush & Lin, 2017). The platform then rises slightly and the heated roller applies pressureto adhere the new layer. The laser cuts the part contour. This process continues until the piece is completed. Extra materials left after the layer is cut remain in place to support the part throughout production (Kumar et al., 2016).

In LOM (Laminated Object Manufacturing) (Figure 3.8), coated paper, plastic foam can be used, as well as ceramic or metal powder-impregnated materials. The easy and cheap availability of the material makes the method advantageous. With the correct selectionof design and parameters, structural and functional models can be obtained in additionto high-precision prototypes of all sizes. Large volume parts can be processed at highspeed. It is an environmentally friendly technology as the material it uses is paper andwater-based adhesive (Klosterman et al., n.d.).

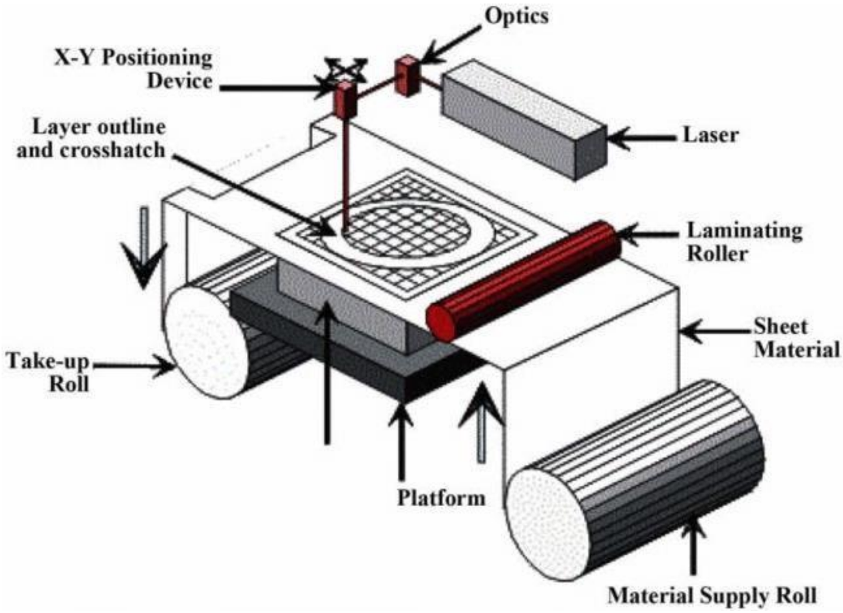

Figure 3.8 Appearance of LOM device (Mantrala et al., 2017).

3.5.4 Polyjet

Polyjet technique is a process that uses inkjet and stereolithography techniques together. In this process, spray heads are used to create each layer. During the process, the model and support materials are sprayed from these heads. These materials are cured with UV light immediately in the spray head. At a time when materials are running out, material cartridges can be easily replaced without interrupting the production process. After the 2D cross-section is cured with UV light in the spray head, the platform descends by 16 µm, the layer thickness. This process of the spray head continues until the part is finished. After the prototype is finished, the support materials can be easily removed from the part with a water jet in a special cabinet (Kechagias & Maropoulos, 2015a; Vidakis et al., 2020).

Polyjet technology, precise and lifelike prototypes can be made with over 100 material types. There are material options such as rubber and hard material, matte and transparent material, high strength and temperature resistant plastic material, dental and medical applications. The device is very easy to use, in Figure 3.9. The tensile strength of the visual appearance. The model material can be processed, chrome plated, glued and used as a master model in mold production. Materials used in this technology is lowerthan other technologies, and should be taken into account when dimensioning the designed geometries than other technologies, and should be taken into account [43-46].

Polyjet technology exhibit full replacement and functional properties with 20% stretch. Since the materials are fully cured, no post-processing is required. The model surface is extremely suitable for applications such as sanding and painting to increase the visual appearance. The model material can be processed, chrome plated, glued and used as a master model in mold production.

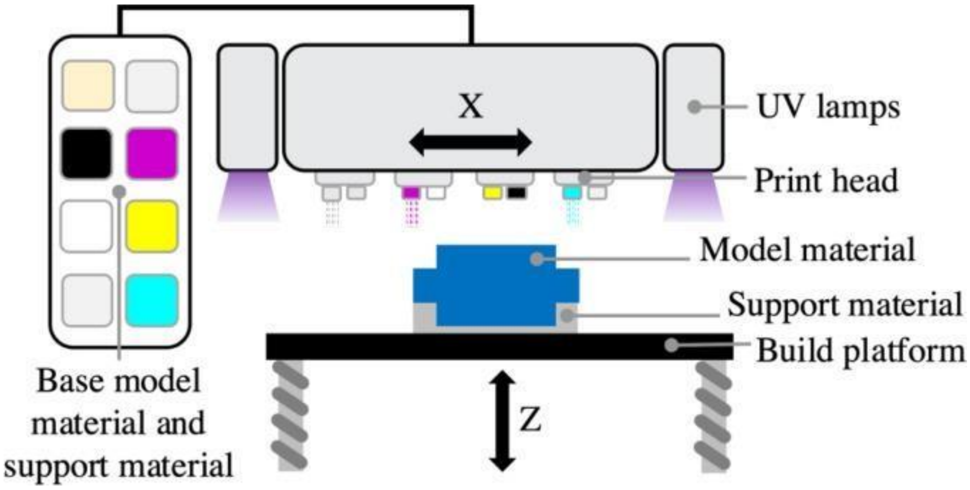

Figure 3.9 Illustration of PolyJet 3D printing(Wei et al., 2022).

Process steps (Kechagias & Maropoulos, 2015b);

- ❖ CAD data and. stl file determine the path that the 3D printer head will move. If necessary, support structures to be used during production are also created at this stage.
- ❖ The photopolymer resin, which is the construction material, is sprayed and cured with UV light and the first layer is formed.
- ❖ Thanks to polyjet materials, which can be chemically cured quickly with UV light, other layers are added to create a model structure.
- ❖ Support materials to be formed as a result of production are cleaned with water and the model is made ready. (Since the support material and the photopolymer resin havedifferent chemical properties, they are sprayed from separate heads.

CHAPTER 4

THEORY OF WEAR

4.1 Introduction

The purpose of this chapter is to review the concept of wear and its types, and to explain the wear that occurs between metal and plastic materials.

4.2 Wear

Wear is an undesirable change in the material as a result of mechanical causes that cause the microparticles to separate from the contacting surfaces (Kato, 2000),(Glodež et al., 1997). There is more than one definition of wear. Wear according to DIN 50320 in international standards, is called as occurring non-desired modifications with deviation of little pieces due to a mechanical cause or energy on the surface of the material (ASM International. Handbook Committee., n.d.). Wear faults are the most frequent and inevitable form of failure mode. Although there are several friction pairs in a machine, they all basically consist of two friction surfaces that move relative to one another. They perform power transformation and transmission so that the machine may carry out a certain movement. Power is inevitably lost during motion, and this lost power degrades friction surfaces bydissipating it as heat and vibration (Amiri & Khonsari M., 2010). The wear rate of a friction pair is practically continually rising if the running-in period is ignored. Early in the wear process, debrisformation causes a progressive roughening of the friction surface, which heightens mechanical vibration. The energy created during asperity deformation heats up the friction surface, thus impairing the metal performance of the wear surface. These two outcomes cause friction wear to worsen, which ultimately results in system failure and component damage. In contact systems, friction and wear are confused with each other. Friction forces cause power loss, and wear prevents the working tolerances fromdeteriorating and the machine parts from fully performing their functions. Wear eventusually; It is seen in shafts, roller bearings, brake pads, engine pistons and cylinders, gears and turbine blades used as motion transmission elements (Figure 4.1). The wear loss, which hasa significant effect on the productive life of different types of engineering materials and machine elements, depends on many factors such as wear environment, wear mechanism, material type, load amount, wear rate, surface film properties formed during friction and temperature.

(a) (b) (c)

Figure 4.1 Wear signs; (a) gear, (b) shaft, (c) bearing surface (Aleksandar Vencl et al., n.d.; Ebersbach et al., 2006; Rivas et al., 2006)

Abrasion is a type of damage where necessary precautions can be taken against other types of damage. Even if the material surfaces in contact with each other are protected by taking precautions like using lubricant, hardening the surface, and forming an oxide layer, mechanical loading and the degrading of the lubricating film or oxide layer due to the heat effect may lead to direct contact between the two surfaces. The material's performance and service life are adversely impacted by the friction that results from this contact. Wear-related damages cannot be eliminated, but they can be reduced by methods including good material pairing, efficient lubrication Figure 4.2 , suitable design, usage of self-lubricating bearings, and filtering.

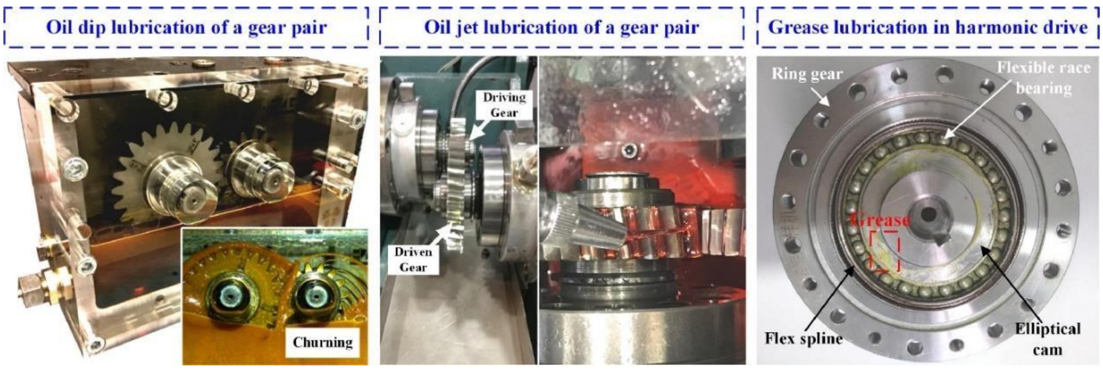

Figure 4.2 Machine elements and lubricants (Liu & Zhu, n.d.)

There are multiple factors that affect wear in operating systems. Some of these factors are factors depending on the main material (crystal structure of the material, hardness, modulus of elasticity, deformation behavior, surface roughness and size), effect of the abrasive, ambient conditions (temperature, humidity), service conditions (pressure, speed, slip path) (Dearn et al., 2013; K D Dearn* & D Walto, n.d.; Wagner & Isaacson, 2019; Wang et al., n.d.).

4.2.1 Factors Effecting Wear

Temperature, shear rate, hardness, elastic modulus, load, and material composition are the key determinants of wear. The contact temperature has an impact on wear resistance (Rymuza, 2007). Abrasive wear would increase because the hardness and yield strengthdecrease with increasing temperature (Xu et al., n.d.). For the majority of the materials, the yieldstrength and hardness decrease with increasing temperature. Metals' yield strength decreases at high temperatures due to the dislocation movement, which facilitates easier plastic deformation. The typical load has a significant impact on wear rate (Lu et al., 2006).The shear force and frictional thrust both increase when more load is applied, hastening the rate of wear (Nuruzzaman et al., 2011). The rate of abrasive wear somewhat increased between0 and 2,5 m/s of sliding speed. The rise in wear may be due to frictional heating. Giventhat wear is also dependent on the force being applied to the surfaces, the availabilityof lubricant, and the surface roughness of the contacting bodies, we cannot generalizethat an increase in sliding speed would necessarily increase wear. A higher value indicates more stiffness, and the elastic modulus is a measure of a material's resistanceto deformation under stress (Sathees Kumar et al., 2021).

4.3 Wear Profiles

Two types of gear tooth contact that are meshed together can be simplified into rolling and sliding with two components. The size of each component is variable from the beginning of the cycle to the end, and with it the size of the components in the rotating and rotating gears change. Although the slip rate and slip speed appear to be identical at the tip and root of the rotating and rotated gears, there is a relative inverse between the slip and the rolling direction.

The rolling and sliding movements of the gears in contact with each other are shown in Figure 4.3. The first contact point is formed by the engagement of the root (tooth root) of the rotating gear and the tip (tooth head) of the rotated gear in Figure 4.3 (a).

The rolling direction is from root to tip for a rotating gear, and from root to root for a rotating gear. However, at the tip of the rotating gear, slip and rolling are in the same direction, while at the root they are opposite. In a rotating gear, the slip direction is always outward from the contact line. In contrast, the slip velocity is from the root to the tip, inward from the contact line (Dhanasekaran & Gnanamoorthy, 2008a).

If the sliding and rolling are in the same direction, it is known as a stop motion. The docking motion can sometimes be more harmful than the stop motion. If the docking situation is more harmful, it is expected that the root part of the rotating gear will wear more than the tip.

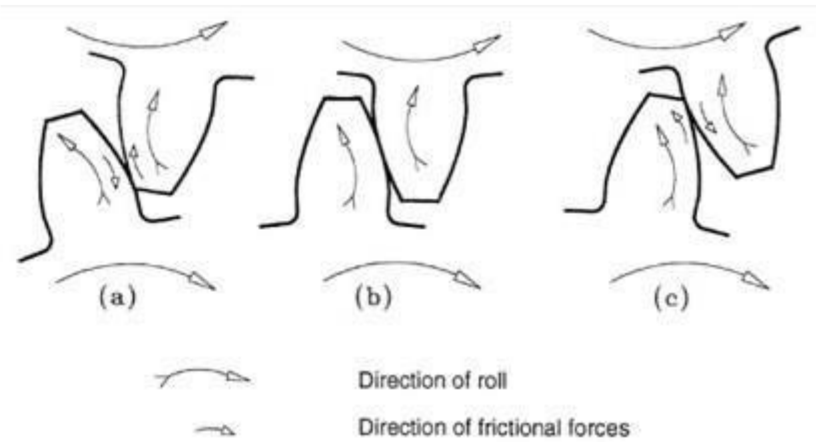

Figure 4.3 Gear tooth contact mechanism: (a) at point first contact; (b) at pitch point and (c) at least point of contact (Dhanasekaran & Gnanamoorthy, 2008b)

Because the lateral and surface dimensions of the rotating and rotated gears are different, slipping occurs continuously at the root and tip. Slip rates of the gears change along the clutch, the rolling circle becomes zero at the point of contact.

Rolling and sliding occur again (Figure 4.3 b) however, the frictional forces are in the opposite direction with respect to the first contact point. The directions of the friction forces due to the sliding motion are shown in Figure 4.3 c. The direction of the friction forces is towards the contact point of the gears in the upper gear (rotating) and outward from the contact point in the lower gear (rotating).

4.4 Wear Mechanism

A tribosystem's settings can affect which wear processes take place. The substance and energy relationship between the components of a tribosystem can be referred to as the wear mechanism. Even when rigid surfaces in contact with each other are shielded by oxide films and boundary lubricants, solid-solid contact still develops owing to the degradation of the oxide film layer under mechanical strain. In this interaction, wear results. Therefore, there is a tangible loss. As a result of the input sizes needed for the start and maintenance of the wear inside the tribological system, several wear processes develop. According to DIN 50320, there are four primary wears that are recognized (Patil et al., n.d.);

- ❖ Adhesive wear
- ❖ Abrasive wear
- ❖ Long life fatigue (phatic) wear
- ❖ Tribochemical Reaction or Tribochemical wear

4.4.1 Adhesive Wear

The form of wear that develops on the surfaces of two materials that are slid together is known as adhesive wear. This type of wear is brought on by the strong atomic binding pressures on the surface of the materials in relation to their surroundings. Strong atomic bonds, covalent, ionic, metallic, or Van der Waals forces at the surface, this attraction starts the separation of the material from one of the surfaces because the bonding is more powerful. The most frequent form of wear, it is characterized by high wear rates and surface friction. Due to contact at the sliding surface interface caused by inadequate surface lubrication, there is considerable adhesion and adhesive wear (Stachowiak & Batchelor, 1993a) is an example of adhesive wear. The molecules of the materials must be broughtvery near to one another in order to generate this force (Yamamoto & Buckley, 1982).

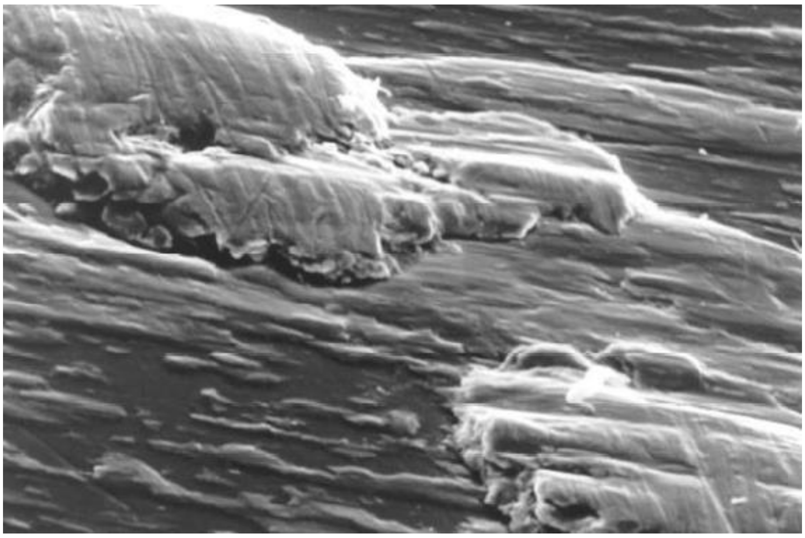

Figure 4.4 Brass film adhesion wear on Alumina (Stachowiak & Batchelor, 1993b)

No matter how sensitive the material's interacting surfaces are prepared, it is a reality that the surface has roughness (indentations and protrusions). In this way, the protrusions between the two surfaces that are in touch allow for contact. The confronting surfaces will never be completely smooth at the molecular level, regardless of how well they are machined or polished. Because of the surface roughness, which makes the real contact surfaces of the two bodies in touch with one another relatively tiny, the pressure from the normal force acting on the actual contact surface is rather high (Gurunathan et al., 2011; HONG et al., 2018; H. Mishina & Hase, 2013; Molinari et al., 2018a; Walton & Goodwin, 1998).

Even with relatively light loads, the stresses at these locations exceed the yield stress limit, and they flow plastically as a result. Microwelds are generated through these plastically deformed surfaces to join objects to one another. The ongoing relative motion between the two objects causes the source interaction to break in the interim. This rupture (Figure 4.4) causes protrusions on the other side, gaps to appear on the soft material object's surface in comparison to the other object, and adhesive particles to spill between of two surfaces (Walton & Goodwin, 1998),(Errichello, 2002; Flodin, n.d.; Molinari et al., 2018b; Podgornik, 2020; Yamamoto & Buckley, 1982).

Adhesion wear happens at some contact sites, not all of them, and occurs between comparable and easily alloyable materials. Abrasion wear (Figure 4.5) is made possible by adhesion wear because it reduces surface roughness and produces sticky particles. Abrasion wear and adhesion wear do not occur simultaneously. When adhesiveparticles are created or when hard particles enter between two surfaces as a result of environmental effects, that is, when the prerequisites for abrasion wear are satisfied, adhesion wear does not take place (Blau & Budinski, n.d.; Finkin, n.d.; Fontalvo et al., 2006; Geitner, n.d.; Molinari et al., 2018b).

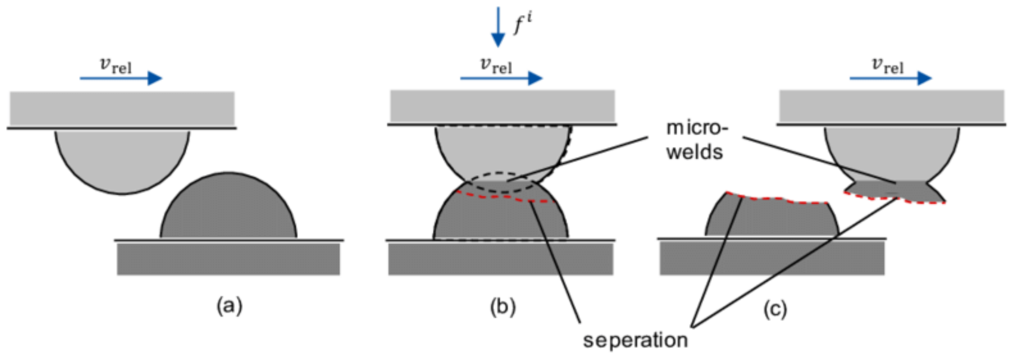

Figure 4.5 Abrasive wear mechanism:(a) before contact; (b) during contact (c) after contact (Terwey et al., 2020).

4.4.1.1 Metal-Metal Adhesion

The adhesion in the case of a metal-metal contact is unaffected by the respective atomic sizes and mutual solubilities of the metals (“The Adhesion of Clean Metals,” 1956). The transfer of material from the weaker to stronger occurs through adhesion when the stronger material comes intocontact with the weaker metal, as shown in Figure 4.6. However, because the metal's surface electrons are not tightly connected to the structure, they can bind with the surface of another metal, which promotes adhesion (Sargent, 1978). Different crystal forms in metals affect how they adhere, and hexagonal closed-pack crystals exhibit less adhesion than other crystal types. Additionally, materials with increased hardness, surface energy, and elastic moduli decrease adhesion (Mokhtar et al., 1980).

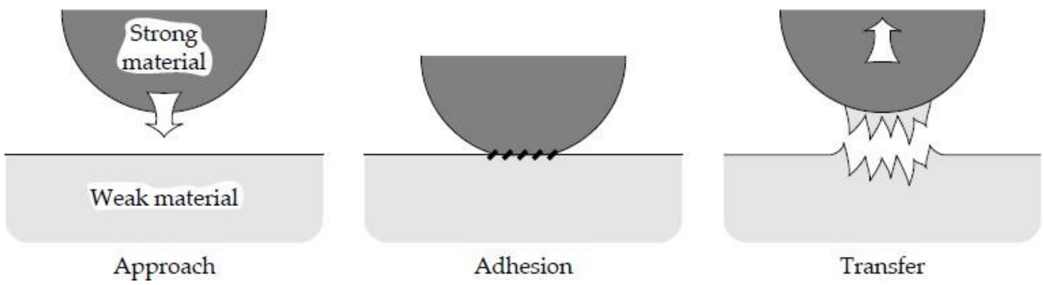

Figure 4.6 Metal transfer procedure involving adhesion (Terwey et al., 2020)

4.4.1.2 Metal-Polymer Adhesion

Metals and polymers both display great adherence, as demonstrated by an extensive series of studies on contact and adhesion of metals and polymers at high vacuum (BUCKLEY, n.d.).

When two materials are separated, adhesion forces between tungsten surfaces and polymers like polytetrafluoroethylene and polyimide are strong enough to transfer the polymer to the metal surface. Reactive non-metals like fluorine have been discovered to have a correlation with adhesion strength (BUCKLEY, n.d.). It is thought that the polymer's surface atoms will connect with the metal's surface atoms, and that this will happen independently of the polymer's inertia. Chemical interactions between the materials cause a strong engagement between metal and polymer (Figure 4.7), and the Van derWaals force of attraction causes a lesser relationship (Briscoe & Tabor, n.d.).

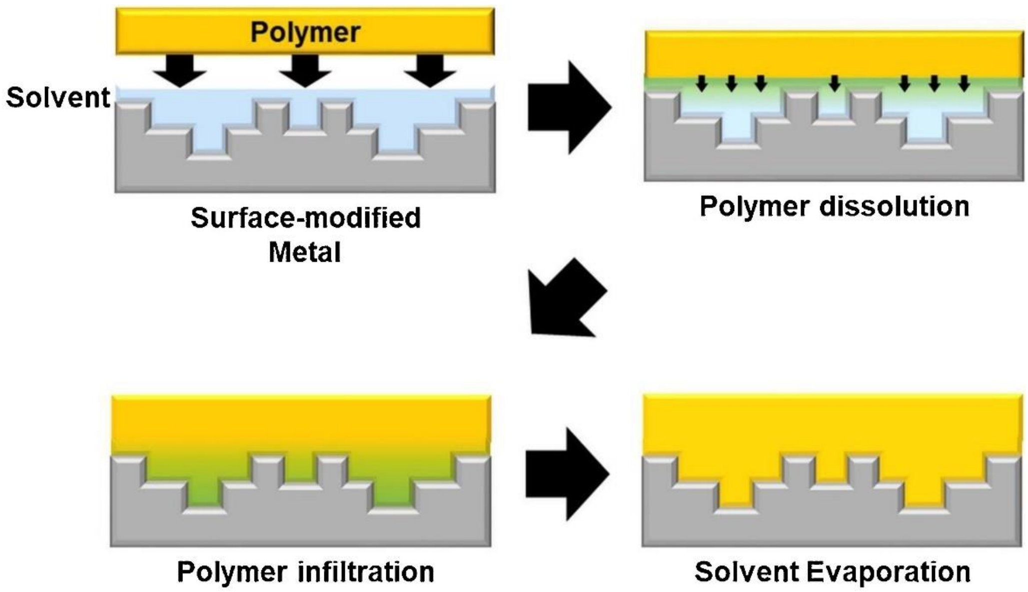

Figure 4.7 Schematic representation of metal- polymer adhesion(Jun et al., 2020)

The mechanism of polymers in metal corrosion is based on strong chemical interactions between metals and polymers. Van der Waals forces are a significant contributor to the frictional resistance of elastomers like rubber, even though they do not directly cause adhesive wear.

4.4.1.3 Transfer-Layer Formation

The hallmark of adhesive wear is the production of transfer layers. Wear particles are created when the transfer layer, which is created as a result of the adhesion of the contacting surfaces, is released. The mechanical alloying that results from the contact of the two metals produces the transfer particle, which is made up of the lamellar surfaces of the two metallic materials (R. A. H. Mishina, 1981). Figure 4.8 can be used to describe the mechanism of transfer layer generation. The first lump, which is the transfer lamellarof the pin and disc surfaces, is created by the sliding action of the pin and disc. The lamellar reaches the necessary size and withdraws from the interface as it slides farther,creating the wear particles.

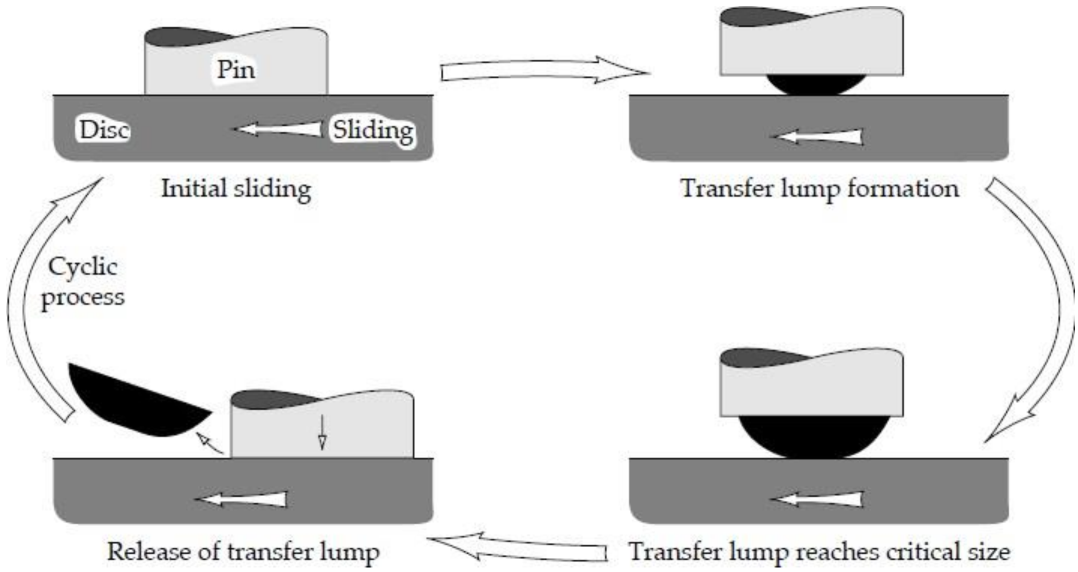

Figure 4.8 Development and elimination of a transfer particle(Terwey et al., 2020)

4.4.2 Abrasive Wear

Scratch wear is another name for abrasive wear. It is a sort of wear that happens when outside hard particles from the environment get between the contact surfaces of two objects that are moving in relation to one another. This wear results in damage to the worn surface in the form of scratches and cuts (MOORE. A. MARTIN, 1978). Sand, scale, rust, machining chips,grinding dust, weld spatter, and wear debris are some of the impurities that induce abrasion in lubricants. It looks like parallel, smooth scrapes or scratches (Figure 4.9) (Errichello, 2002).

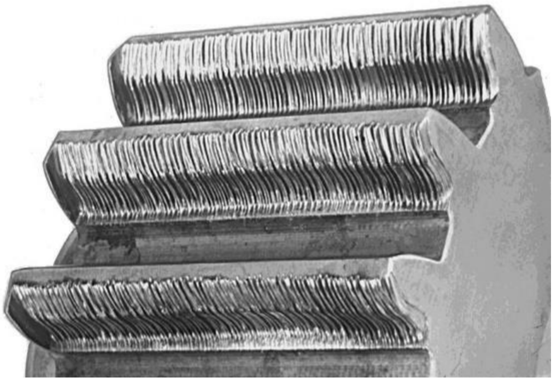

Figure 4.9 Excessive abrasion type wear (Stachowiak & Batchelor, 1993a)

There are two forms of abrasive wear; "two-body abrasive wear" (Figure 4.10) refers to damage caused by chips being removed from the surface of the opposite item when one of the two objects in touch has a rougher surface that is harder than the other as a result of relative movement and contact pressure (Rabinowicz et al., n.d.).

Three-body abrasive wear (Figure 4.10 c) is the term used to describe the type of wear that occurs when abrasive particles may freely travel between two bodies (i.e., they can perform both translational and rotational motions). There could be evidence of worn chips, or these particles could infiltrate the interface from the outside. Due to interfering dust, mineral grains, abrasive chip residues, or oxide particles remaining as a whole, wear often begins as a two-body abrasive or adhesive and eventually progresses to a three-body abrasive (Petrica et al., 2013).

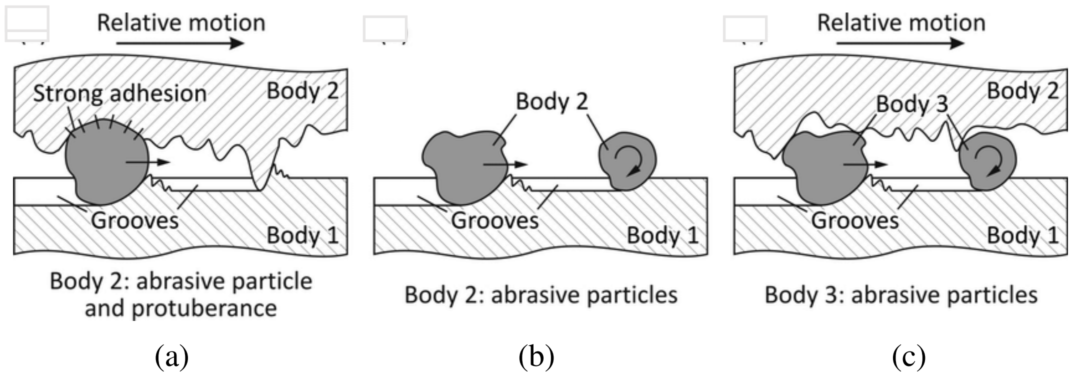

Figure 4.10 Two and three body abrasive wear (Kandeva et al., 2016)

Causes of Abrasive Wear Mechanisms:

(a) **Micro cutting:** With great machining accuracy and excellent surface quality, microcutting is a precise process that allows for flexible creation of microfeatures or intricate three-dimensional components.

(b) **Micro-fracture:** The merging of several smaller fractures leads to the fracture of the worn surface.

(c) **Micro fatigue:** It is a small-scale fatigue damage brought on by recurrent loads or ongoing gear rotation. The material develops microcracks as a result of this damage. Material choice, gear shape, and appropriate lubrication are a few examples of the causes of microfatigue. To prevent damage, the right material, surface hardness, thread profile, and lubrication system are necessary.

(d)**Removal of material grains:** It involves the abrasion or removal of material grains from gears. It is a machining technique that is typically applied to give a more accurate machining of the surface or to boost the smoothness of gear surfaces.

4.4.3 Fatigue Wear

There are several ways that gears might malfunction, and except an increase in noise and vibration, there is frequently no warning before catastrophic failure. In general, each type of failure leaves distinctive traces on gear teeth, and careful inspection frequently provides enough details to determine the reason of failure. Fatigue, impact fracture, wear, and stress rupture are the common failure mechanisms (in decreasing order of frequency) (Fernandes, 1996; Senophoe & Yadav, 2012).

The most frequent gearing failure is fatigue. Two of the most frequent forms of fatigue failure in gears are tooth bending fatigue and surface contact fatigue. Fatigue failure has a number of known causes. These include improper substance and heat treatment usage, improper gear assembly or misalignment, overloads, unintentional stress raisers, subsurface faults in crucial regions, and bad gear set design (Zmitrowicz, 2006).

While there is continuous contact in adhesive and abrasive wear, a different wear mechanism emerges in cases of cyclical contact. Pitting wear is a common phenomenon in surfaces that are in constant contact with each other, such as gear wheels, rolling bearings and cam mechanisms type of wear (Figure 4.11). For rotating structural members, there is usually anelastic contact between the parts. At the contact point, the main wear mechanism is high cycle fatigue wear.

Figure 4.11 Appearance in general of the damaged helical gear (Asi, 2006)

Since the contact areas in such machine elements are very small, Hertz pressures occur on the contact surfaces. Under the influence of these pressures, shear stresses occur just below the surface. At the point where shear stresses are maximum, plastic deformation occurs and this deformation progresses to the surface over time and pits occur on the surface (Figure 4.12) (Liu et al., 2020). Pitting is a three-dimensional phenomenon that is highly influenced by the finish of the contact surface, the microstructure of thematerial, and the operating circumstances, such as the kind of contact, the stress, the misalignment, the lubrication, the temperature, etc. In general, spalling is seen as a continuation or propagation of rolling contact fatigue and pitting rather than an initiating mechanism of failure. Although spalling shows as deeper voids at contact surfaces, pitting appears as shallow craters (Fernandes, 1996)100].

Natural hardness is a crucial factor in this kind of wear. Soft fabrics do not experience fatigue wear. Surface hardening is the best defense against fatigue wear (Johnson, 1989).

Figure 4.12 Macro pitting failure on gear tooth (Sun et al., 2017)

4.4.4 Tribochemical Reaction or Tribochemical Wear

As a result of a chemical interaction between the material surface and the corroding medium, which can be chemical agents, lubricants, or air media, the material surface disintegrates in a kind of wear known as corrosive wear. The wear is accelerated by the rise in temperature. The material should be covered with a protective covering if you want to avoid this wear. This is a general word for wear that refers to any wear brought on by corrosion or a chemical reaction.

The material undergoing this wear would suffer substantial damage or material loss since it is characterized by both wear and corrosion processes (Stachowiak & Batchelor, 1993a). Figure 4.13 depicts the bearing surface's corrosive wear.

Figure 4.13 Bearing surface damaged by corrosive wear (Aleksandar Vencl et al., n.d.)

Corrosive wear happens when the worn surfaces are additionally subjected to corrosive effects, moisture and oxygen are the main causes of corrosion in the atmosphere. In addition, corrosive media include aqueous solutions, bases, acids, molten salts, liquid metals, and inorganic solvents. For usage in a freshwater environment, metals including steel, aluminum, cast iron, copper, and certain stainless steels are better choices. It is possible for chemical corrosion to happen on its own or in conjunction with other kinds of wear based on the touching surfaces' surface film.

The chemical reactions created prevent surface wear. However, if the surface film formed is fragile and the interfacial bond is weak, the films crack and separate from the surface during friction and the wear rate increases.

Depending on the kind of media supporting the corrosion process and the presence of corroding elements, the mechanism of corrosion may be described in several ways. The following kinds of interaction between the corrosive agent and the worn surface can be seen when a material contact in a sliding situation in a lubricating medium is experiencing corrosion.

The corrosion-prone material may experience surface alterations that result in the development of a lubricating coating on the surface. A protective thin coating arises if this lubricating film prevents the effects of adhesion and corrosion. However, these kinds of protective films formed by the corrosion products are very rare. The schematic representation of this mode can be seen in Figure 4.14-a.

By serving as a sacrificial layer, the film that is created as a result of the corrosion products can inhibit adhesion. However, corrosive wear can occur, and these films can be visible when brittle oxides or ionic chemicals are present. The schematic representation of this mode is shown in the Figure 4.14-b.

Rapid corrosion formation causes the protective thin coating to totally wear down, leaving surface figures and pitting. Large pitting causes anodic dissolution to occur on the surface, which intensifies corrosion on the medium. The schematic representation of this mode is shown in the Figure 4.14-c

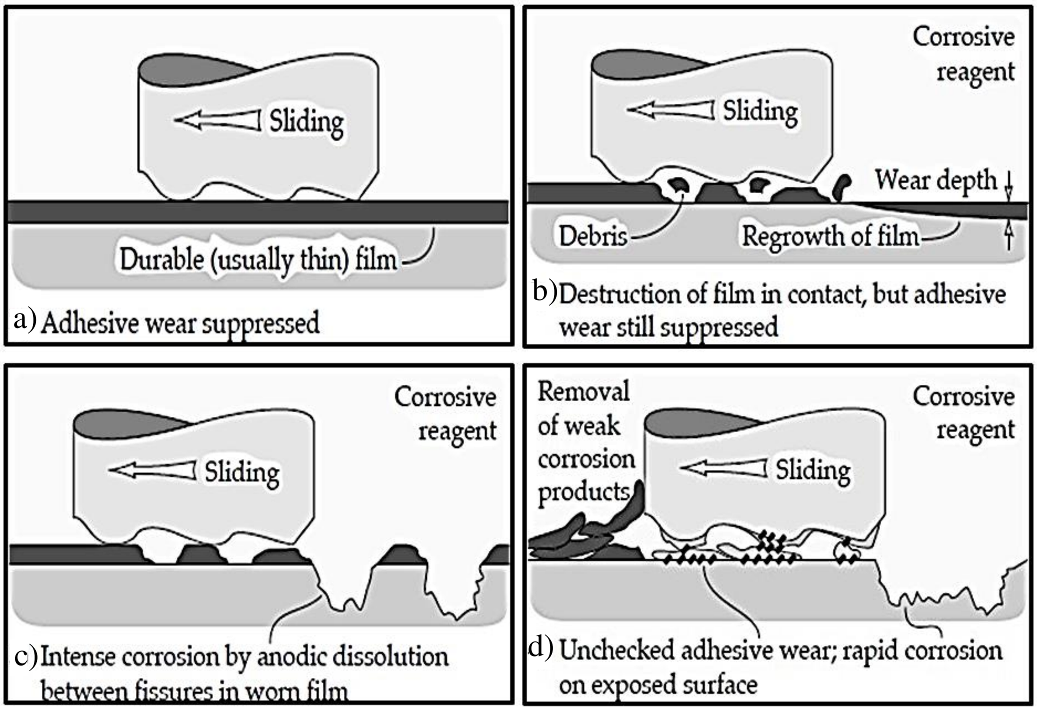

Figure 4.14 Tribochemical Wear shown(Stachowiak & Batchelor, 1993a)

If the corrosion coatings are sacrificial, they cause eventual loss owing to mechanical agitation on the surface medium while initially shielding the surfaces from corrosion and adhesion. Modeling the film formation process allows for the prediction of wear performance over time.

Corrosion and wear may be separated because the corrosive chemicals that are produced are weak and soluble in liquids, which allows wear and corrosion to work separately on surfaces. There are areas where adhesive wear is more common, and in other areas, corrosion has advanced (Hsu & Klaus, 1978). This mode is shown the Figure 4.14-d.

The major characteristic of corrosive wear is the creation of corrosion films, as is evident from the corrosive wear formation mechanisms. The corrosion films that are originally generated shield the surfaces from both corrosion and adhesion; however, if the corrosion film is a bouncer film, this produces additional losses since it agitates the surface medium mechanically. It is possible to simulate the film production processto forecast wear performance over time (Yahagi & Mizutani, 1984).

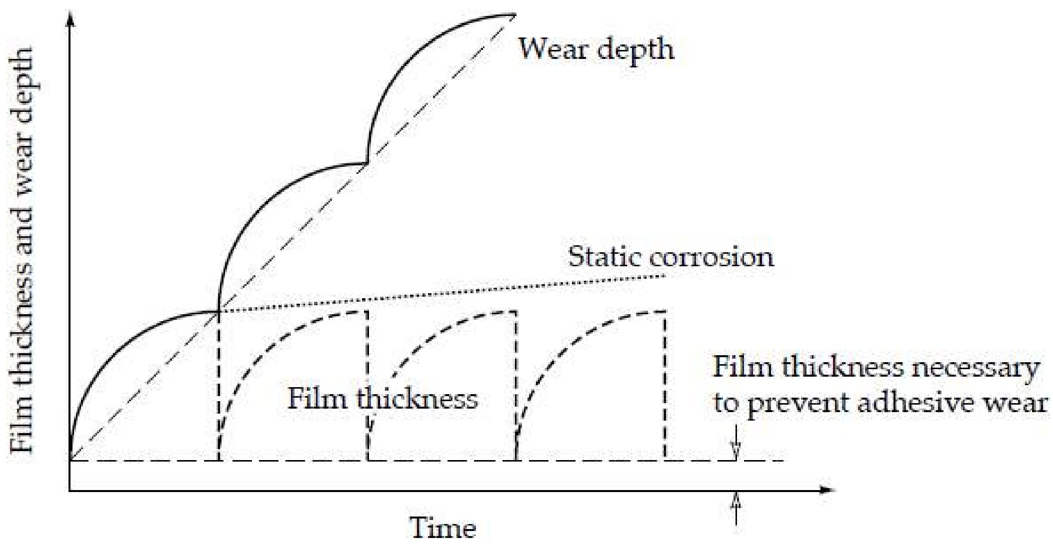

Figure 4.15 Corrosive wear model that explains the protective film (Klosterman et al., n.d.)

The graph of film thickness / wear depth vs time is shown in Figure 4.15. The creation of the passivating coating, which has a certain thickness and maintains the steady corrosion wear, occurs throughout the progressive rise in time in corrosive wear. However, beacuse of the rise in friction temperatures brought on by sliding, this film can not develop (Mcdonald & Stott, 1987).

To lessen surface wear, the effects of lubricants on the materials' surfaces are necessary. As the protective coating forms and the lubricating medium's reactivity is decreased, there is a decrease in the adhesive wear in corrosion wear. As a result, the lubricant's reactivity is dependent on how corrosive the surface is; as corrosivity rises, lubricant reactivity also rises, which inhibits the creation of the protective coating and results in increased adhesive wear rates. To balance the wear rates of adhesive and corrosive materials, it is crucial to optimize the lubricant's composition (Klaus & Bieber, 1964).

4.4.4.1 Corrosive and Adhesive Wear Transition

By reducing the corrosiveness of the medium, it can be converted into a suitable lubricant at a given load and sliding speed. However, severe adhesive wear can occur if the corrosiveness or reactivity of the lubricant is severely reduced due to poor development of surface protective coatings. As shown in Figure 4.16, the lubricant composition can be adjusted to balance corrosive and adhesive wear and minimize the wear rate.

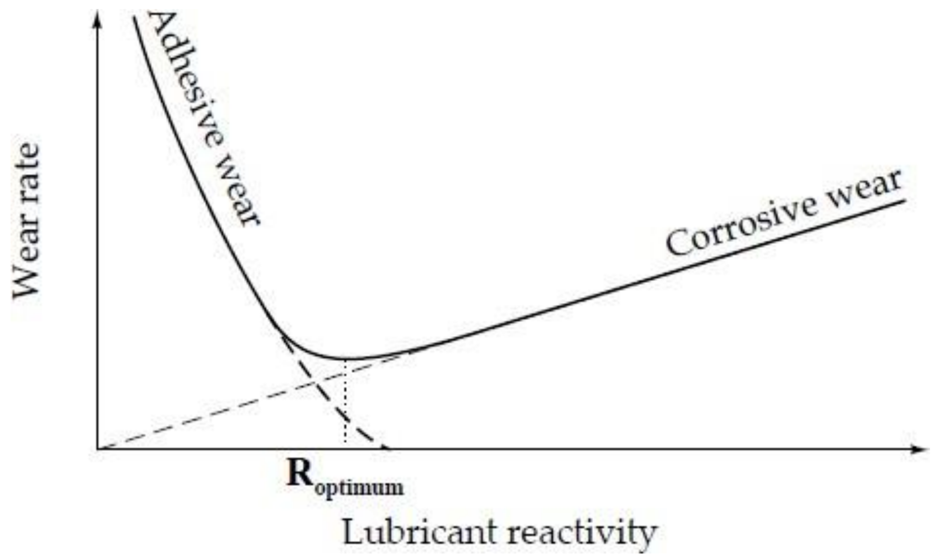

Figure 4.16 Wear rate vs lubricant reactivity graph (Stachıwiak W.Gwidon & Batchelor W.Andrew, 1993)

Two distinct wear processes that take place during material wear are referred to as corrosive and sticky wear transition. It is the wear incidents that result from friction and abrasion on the workpiece's surface. Movement between the contacting surfaces creates friction on the workpiece, which separates material particles or wears away the surface.

The term "corrosive wear" describes how a material's surface deteriorates due to chemical reactions. Chemicals (acids, bases, salts, etc.) acting on the surface of the material can cause the material's particles to separate and the surface to wear, especially in hostile settings. Pits, grooves, or surface degradation resembling pits may result from this process. It happens frequently that materials corrode, especially metallic ones.

CHAPTER 5
EXPERIMENTAL STUDIES

5.1 Introduction

In this section, the production of plastic gears (PA6 and PEI) used in the experiments and the equipment, devices and features used in the measurements and analyzes as a result of the experiment are explained in detail

5.2 Experimental Set-up

Gear wear tests were carried out at different speeds and torque values of approximately 3 Nm while they are meshed. Figure 5.1 illustrates the gear testing machine in detail. It is also shown schematically in Figure 5.3 . A servo motor (4.5 kW) was connected to both PEI and polyamide gears that were being tested and they were mated to a steel gear. The gear test rigs were loaded with test gears, which were either PEI gears made through 3D printing or machined polyamide gears. The gears were subjected to a specified level of loading through either torque or rotational speed. The testing of the 3D printed PEI gears was conducted in the same way as that of the machined polyamide gears.

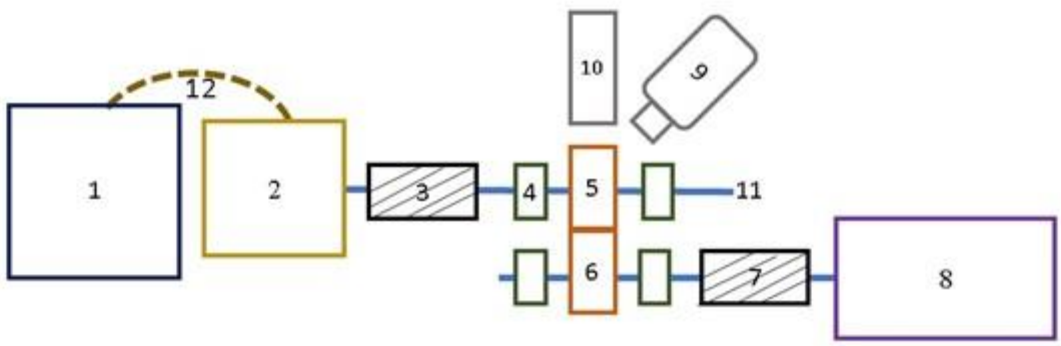

Figure 5.1 Schematic representation of test rig

1. Torque measuring system	2. Servo Motor	3. Coupling	4. Roller bearing	5. Driving gear	6. Driven gear	
7. Coupling	8.Electromagnetic dust brake		9. Noise meter	10. Temperature sensor	11. Shaft	12. Cables

Figure 5.2 Equipments of test rig

The wear tester was then changed and a loading arm was added to the driven gear, these gears will be operated under different torques until damage occurs to the gears. When the literature is examined, damage occurs in plastic gears in the range 10-12 and 15 Nm are obtained and damage occurs in the PA6 and Ultem 1010 gears at 800 rpm.

The movement starts from the shaft connected to the servo motor and the drive gears are PA6 and Ultem 1010. The wear tests were performed at 400 rpm, 800 rpm and 1200 rpm speeds and the plastic gears completed $10x10^5$ cycle at these speeds.

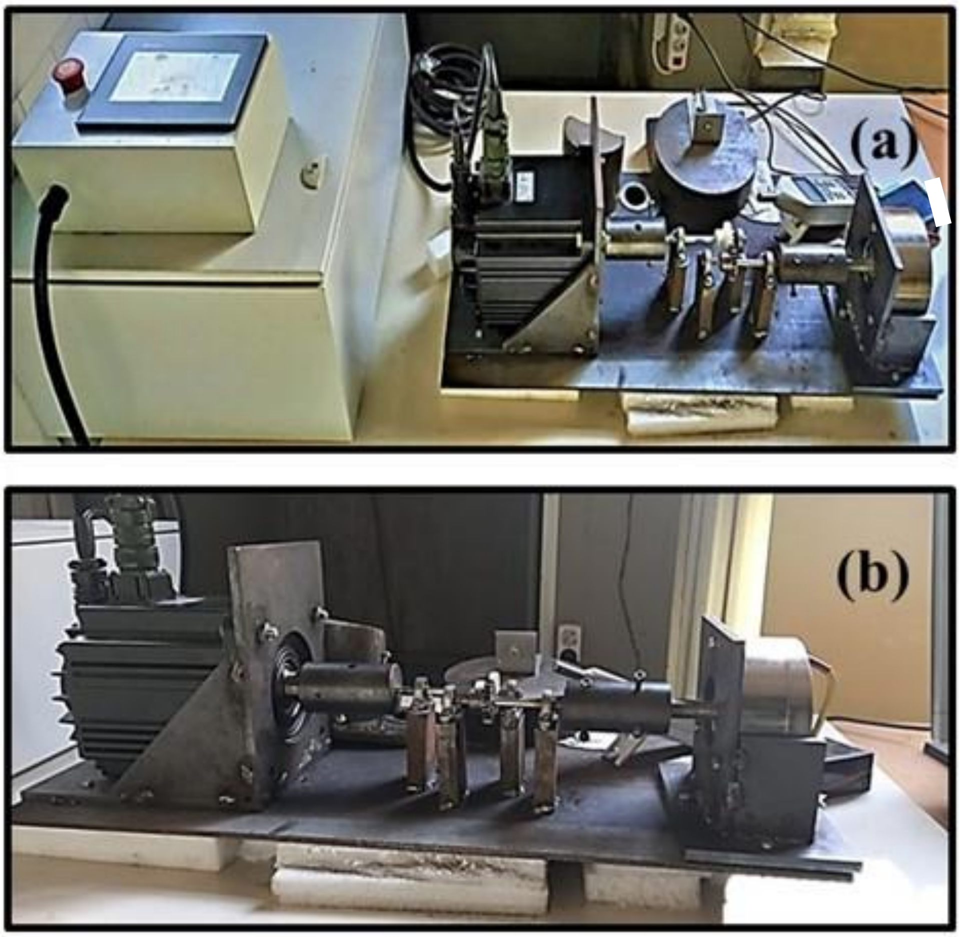

Figure 5.3 Testing rig;(a) top view, (b) front view

The test was performed by operating the gears at three different rotational speeds while keeping the torque at 3±0.5 Nm, as seen in Figure 5.4 . The aim of this study is to compare the durability and wear performance of PEI and polyamide gears by running them until they break.

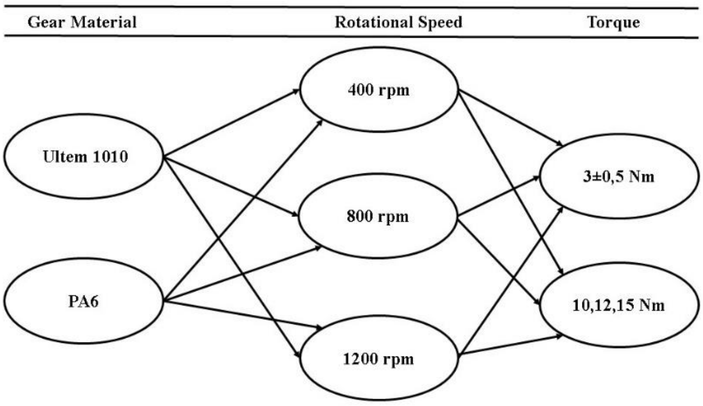

Figure 5.4 Flow diagram of speed and torque

(a)

(b)

Figure 5.5 Wear tester for torque experiments

Another phase of the wear tests is to run the PA6 and Ultem 1010 gears at 800 rpm and 1200 rpm until they are damaged. When the literature is examined, there are wear tests in the range of 10 Nm, 12 Nm and 15 Nm torque at 800 rpm and 1200 rpm. In order to obtain the torque at these values, a disc is attached to the shaft with the driven gear, and a loading arm is placed on this disc.

5.3 Test Measuring Equipment

In addition to the speed and torque factor changes, 2 different gear types are used, and the torque values change due to temperature, wear, surface roughness, noise and the structure of the gears. In each experiment, second-second temperature, sound intensity and torque values were recorded with measuring devices. The amount of wear and surface roughness were measured every 200,000 cycles. The details of the devices used are described under this heading.

5.3.1 Sound Level Meter

A sound measuring device was used to determine the sound intensity during the experiments. The model of the device used is Lutron SL-4033SD. It is shown in Figure 5.6. Having an SD card made it easy to use data and create graphs. Also, no software is needed for this device. The frequency band range is 31.5 Hz ~ 16 kHz. It works with 6 *1.5volt batteries. After the data is saved to the computer, the format is made to the voice recorder.

Figure 5.6 Sound level meter (Lutron SL-4033 SD)

5.3.2 Temperature Measuring Device

Very high temperatures were obtained during the experiments, especially for the PA6 gear. We will examine these results under the heading of results. Temperature values were measured and recorded with a Micro-Epsilon cs-sf15-c3 model device. It is shown in Figure 5.7.Measuring range -20°C to 350°C. The wavelength is in the range of 8-14 μm. Output voltage is in the range of 5-30 vdc. It is shown in Figure 5.8. A software is required for this device. After the software is installed on the computer, it shows the temperature change on the screen.

Figure 5.7 Micro-Epsilon Cs-Sf15-C3

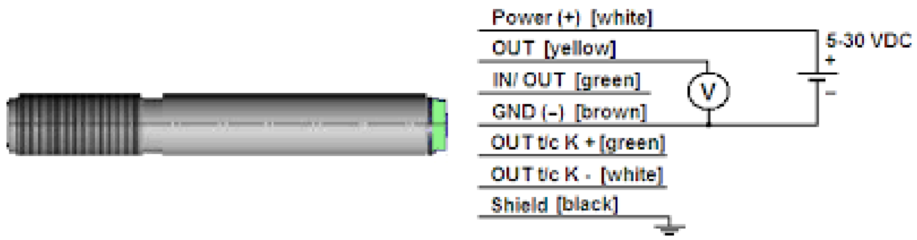

Figure 5.8 Analog device

5.3.3 Surface Roughness Digital Measuring Device

Before starting the wear tests, the surface roughness values of the gears were measured. Afterwards, surface roughness values were checked every 200,000 cycles. These measurements were made with Mitutoyo- SJ 410 model device. It is shown in Figure 5.8 . The SJ-410 is a desktop type surface roughness and waviness measuring instrument that monitors the surfaces of different machine parts, calculates surface roughness based on roughness standards and displays the results. The detector tip of the SJ-410 monitors for minor irregularities on the workpiece surface. Vertical tip deflection and horizontal movement are processed and displayed digitally on the SJ-410's touchscreen during monitoring. Wide measuring range and different roughness parameters. It has a maximum range of 800 µm (±400 µm) and can display different roughness parameters about surface roughness.

Figure 5.9 Mitutoyo SJ-410

Surface roughness values were measured from the face of the gear (Figure 5.11). The measurements were made in 4 different gear profiles (Figure 5.10 a), and 4 measurements were taken from each gear cheek, and the arithmetic average of all measurements was recorded as the roughness value. The wear depths of the gears were determined by measuring the roughness of the tooth profile as Ra.

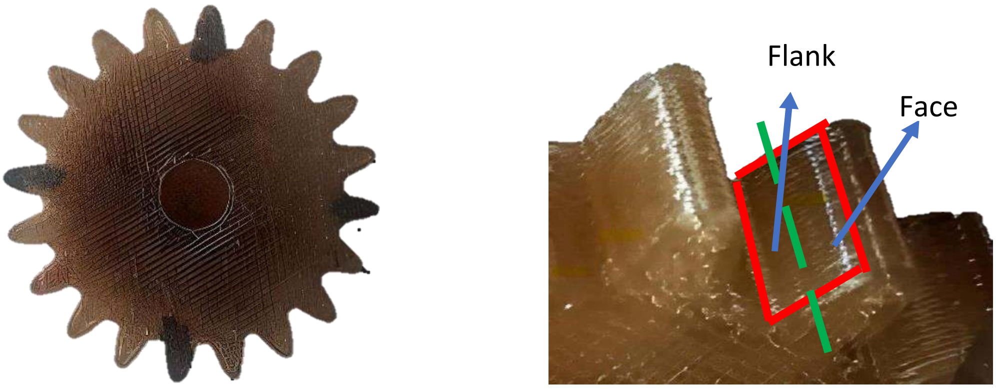

(a) (b)

Figure 5.10 (a) Ultem 1010 spur gear, (b) face and flank on the tooth surface

The surface of the gears is divided into 2 parts as face and flank. Face; It is the toothed surface between the section circle and the addendum circle. Flank is; It is the toothed surface between the division circle and the dedendum circle. In gears, the contact takes place in the face part(Rana et al., 2023; Y. Zhang & Fang, n.d.).

Therefore, the surface roughness is measured from the face part. The face and flank parts are shown on the surface of the Ultem 1010 gear in Figure 5.10-b.

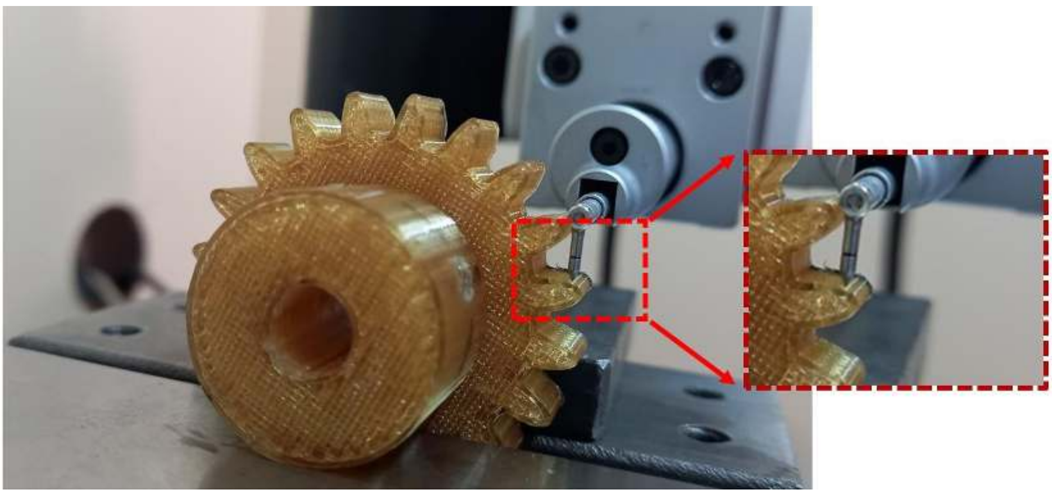

Figure 5.11 Surface roughness measurement from the face section

Figure 5.11 shows where the pointer of the surface roughness device is. Roughness values were measured from the face surfaces of Ra, PA6 and Ultem 1010 gears. Also, Figure 5.12 shows the direction of movement of the surface roughness needle and the Ra values are measured precisely by moving the needle back and forth.

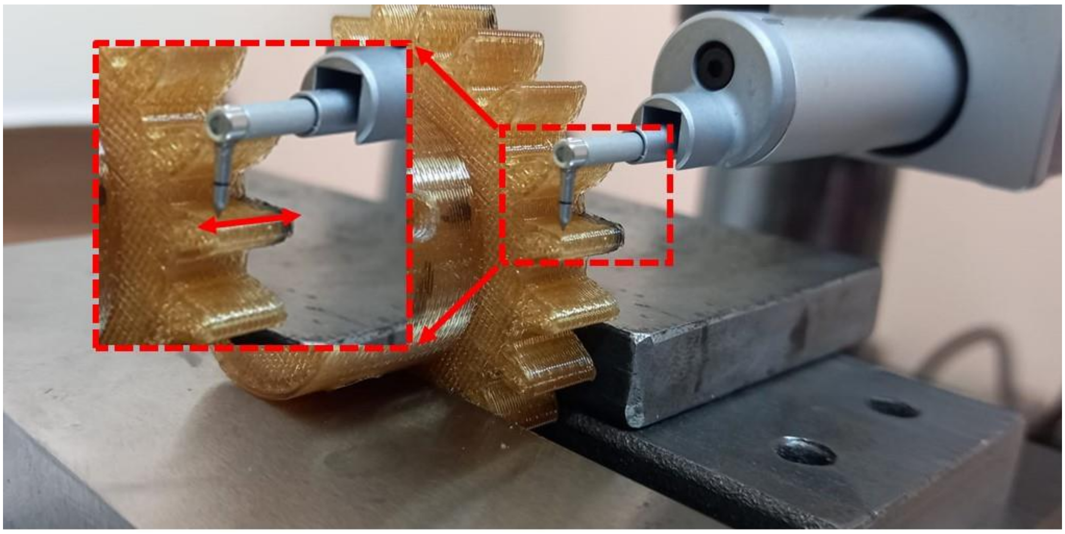

Figure 5.12 The direction of movement of the needle is shown.

5.3.4 Weight Measurement

RADWAG Wagi Elektroniczne brand precision balance was used to test tooth profile damages with electronic scales. The initial weights of the gears were measured before they were subjected to the wear test, and then their weights were measured again in every 200,000 cycles. With this method, the amount of wear was obtained according to the initial situation.

Figure 5.13 Precision scales for weighing gears

5.4 Gear Manufacturing Process

5.4.1 Formation of Ultem 1010 Spur Gear

The Ultem 1010 gear was modeled in Solidworks and then converted to 3D printing using the Ultimaker software program. This software works by dividing the model file into layers and generating a printer-specific G-code. Once complete, the G-code sends the physical object to the printer for production.

The Stratasys Fortus 450mc 3D printer was used to produce Ultem 1010 gears with all process parameters set to their default values. The Stratasys Fortus 450mc 3D printer is shown in Figure 5.14. The maximum part size of the printer is 406x355x406 mm and the layer resolution is ±127 µm. Gears are properly printed, including air gap, build direction, raster angle, print speed, counter and stroke count. The resulting Ultem 1010 samples were fabricated using a +45°/-45° scanning angle with 100% fill density and layer thicknesses of 330 µm.

Figure 5.14 Stratasys Fortus 450mc 3D printer

Table 5.1 show the material properties of the Ultem 1010 gear.

Table 5.1 Features of Ultem 1010 spur gear

Density (g/cm3)	1.27
Tensile strength, yield (MPa)	64
Glass transition temperature (°C)	215
Thermal conductivity (W/m-K)	0.22
Coefficient of friction	0.30

The tooth profile properties of AISI 1040 steel gear, Ultem 1010 and PA6 gears used in this study are shown in Table 5.2. Instead of AISI 1040 steel, alternative steel gears could be preferred.

Table 5.2 Gear Profile

	AISI 1040 / PEI / PA6
Module	2
Number of teeth	20
Pressure angle (°)	20
Face width (mm)	8
Hub diameter (mm)	20

Figure 5.13 shows the pre-production model of the Ultem 1010 gear on the 3D printer and the Ultem 1010 gear 3D printed after the production. Also, the raster angle and infill density are highlighted in Figure 5.15.

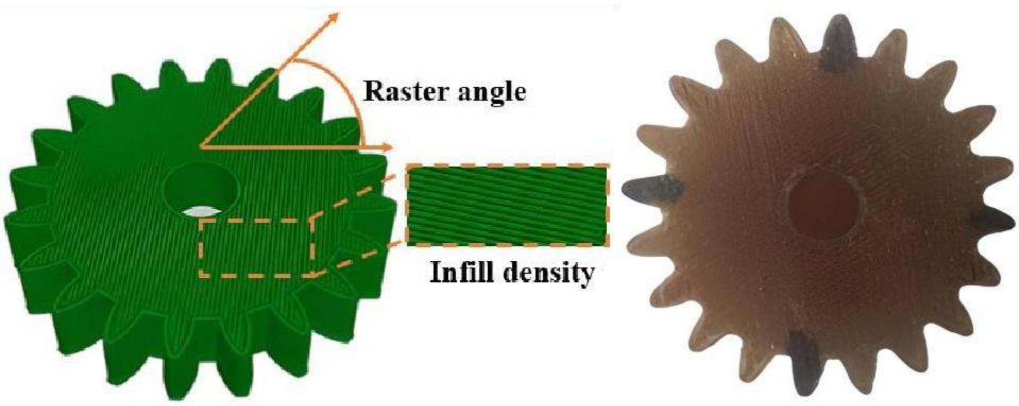

(a) (b)

Figure 5.15 (a) 3D model gear, (b) 3D printed gear

Layer thickness of Ultem 1010 gear is 330 µm and raster angle is produced as ±45°. Higher layer thickness means better strength. When the raster angle is 45°, it shows that the friction force will be lower during the tests (Amirruddin et al., 2021). In Figure 5.14, different raster angles are shown for clarity.

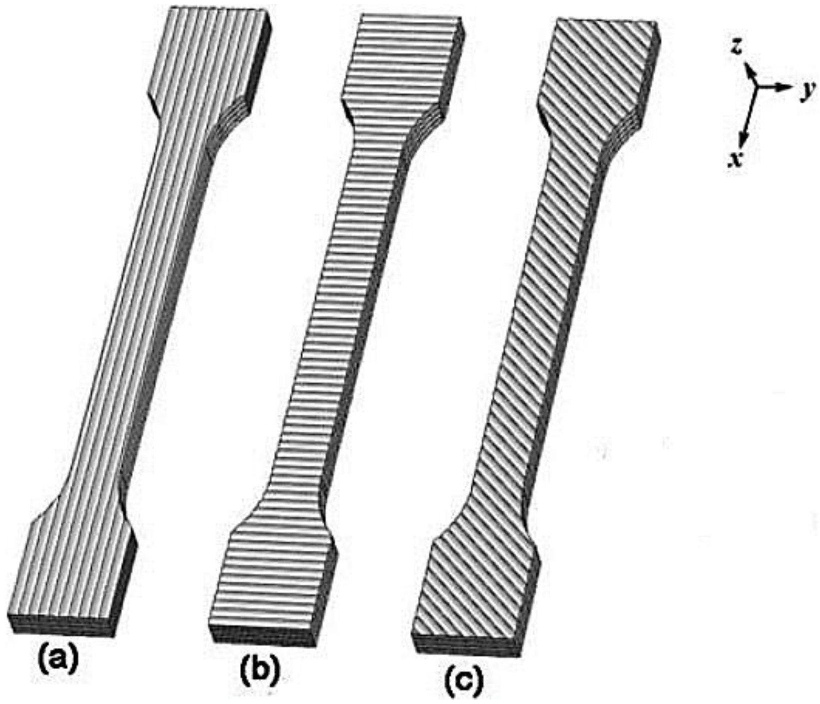

Figure 5.16 Different alignment orientations. (a) 0° raster angle, (b) 90° raster angle, and (c) ±45° raster angle (Jiang et al., 2019).

Table 5.3 Features of PA6 spur gear

	PA6
Density (g/cm3)	1.14
Tensile strength, yield (MPa)	70
Glass transition temperature (°C)	60
Thermal conductivity (W/m-K)	0.28
Coefficient of friction	0.82

5.4.2 Formation of PA6

Machining is a widely used manufacturing method for shaping metal or plastic parts. In this method, CNC (Computerized Numerical Control) machine, which is a machining technique, is used. PA6 is a known thermoplastic and is a widely used engineering plastic in the industry. The design and modeling of the PA6 gear part was done using CAD (Computer Aided Design) software. PA6 is a preferred material for gear manufacturing due to its favorable strength properties, low coefficient of friction and high wear resistance. PA6 bars (Figure 5.17) were cut on the CNC machine. The machine tool is programmed to accurately cut the dimensions and shapes of the gear piece. The cut PA6 bars were milled on a CNC machine to take the shape of the gears. The milling process ensures accurate cutting of gears. After the milling process was completed, the surfaces of the gears were smoothed. The surface roughness of the PA6 gear was measured from the marked points on its teeth every 200,000 cycles. Table 5.3 show the material properties of the Ultem 1010 gear.

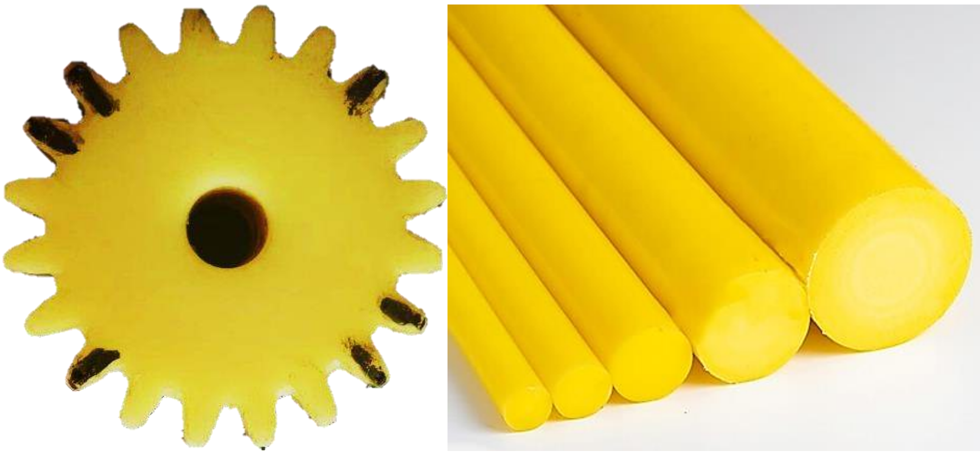

(a) (b)

Figure 5.17 In shown PA6 material. (a) PA6 bars, (b) PA6 gear

CHAPTER 6
RESULTS AND DISCUSSION

6.1 Introduction

This section contains the results and interpretation of wear tests at 3±0.5 Nm torque and at different speeds. Initially, experiments were carried out at 400 rpm, 800 rpm and 1200 rpm in both gears and a torque of 3Nm ± 0.5 Nm. Torque was tried to be kept constant. Weight and roughness measurements were made every 200,000 revolutions at all speeds. Torque, temperature and noise values occurring during the experiments were measured and recorded. Both gears, PA6 and PEI, completed 1,000,000 cycles against the steel gear.

We will examine these results under subheadings as wear results, surface roughness results, thermal analysis and noise results.

6.2 Wear Results

The wear difference between the plastic gear and the steel gear is due to the different properties of gear materials. Plastic gears have lower density, lower stiffness and less wear resistance than steel gears. At the same time, plastic gears have lower thermal conductivity than steel gears and are less resistant to high temperatures.

As the speed increases, the contact speed of the gears also increases. This can cause more heat and wear on the gears. Because plastic gears are less durable than steel gears, they may experience faster wear when used at high speeds.

Also, as the speed increases, the load applied to the gears also increases. This can cause the gears to operate under more stress and therefore wear faster.

As a result, increasing speed can increase the amount of wear on the gears and can also increase the load applied to the gears. Due to the lower durability of plastic gears than steel gears, they may experience faster wear when used at high speeds.

Table 6.1 and Table 6.2 are show the wear rates of gear pairs at different speeds, 400 rpm, 800rpm and 1200 rpm, every 200,000 cycles.

Table 6.1 The amount of wear of the PA6 gear is shown.

Cycle * 10^3	400 rpm	800 rpm	1200 rpm
	Weight (g)		
0	18,35	18,42	18,35
200	18,28	18,33	18,32
400	18,27	18,27	18,25
600	18,25	18,26	18,23
800	18,21	18,24	18,21
1000	18,20	18,22	18,13
Total loss	0,15	0,20	0,22

Table 6.2 The amount of wear of the Ultem 1010 gear is shown.

Cycle * 10^3	400 rpm	800 rpm	1200 rpm
	Weight (g)		
0	18,33	18,17	18,25
200	18,13	18,05	18,22
400	18,07	17,96	18,21
600	18,01	17,92	18,17
800	17,98	17,91	18,14
1000	17,94	17,88	18,06
Total loss	0,39	0,29	0,19

Table 6.1 and Table 6.2 show the losses occurring in gears every 200,000 cycles from the initial state to 1000000 cycles at 400 rpm, 800 rpm and 1200 rpm speeds. It continues as 0.15 g, 0.20 g and 0.22 g for the PA6 gear. From here, the following conclusion should be drawn; As the speed increased, the contact of the tooth surfaces with each other increased and the amount of wear increased as well.

For the Ultem 1010 gear, the total wear amount is 0.39 g at first, and it is seen as 0.19 after 1200 rpm. Here is the result; There is a trend showing that the wear of the Ultem 1010 gear at high speeds is getting less and less. This trend is shown in Figure 6.1. In terms of wear performance, Ultem 1010 showed a better result.

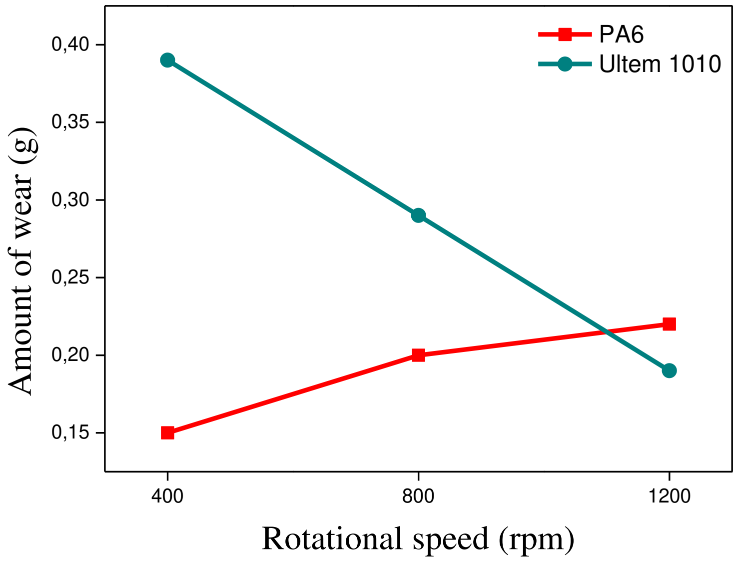

Figure 6.1 The wear trend of PA6 and Ultem 1010 gears are shown

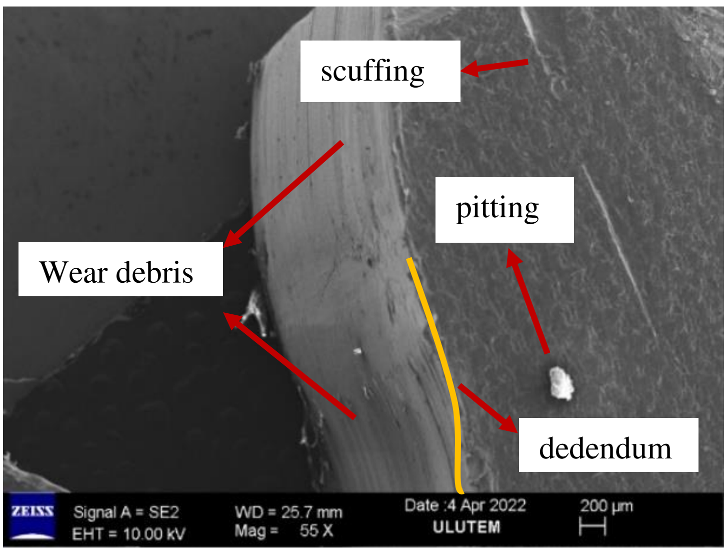

(a)

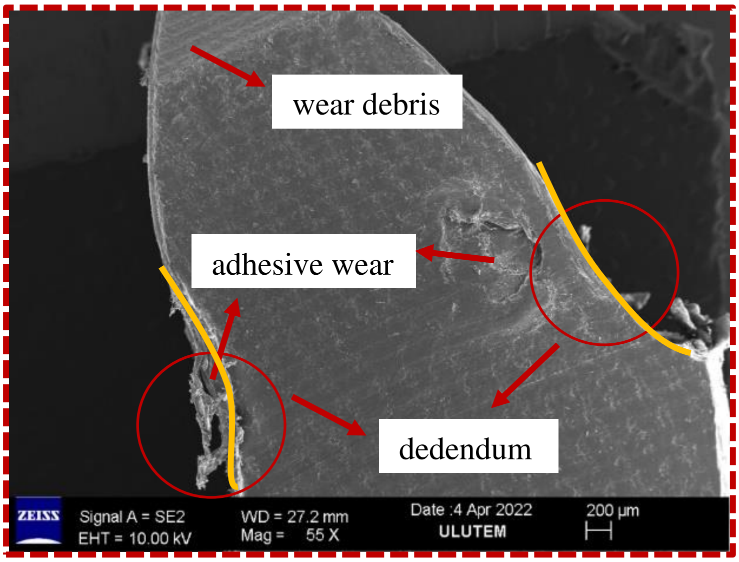

(b)

Figure 6.2 SEM images of PA6 gear (x55); (a) at 400 rpm, (b) at 800 rpm

As a result of the PA6 gear working at 400 rpm and 800 rpm, images were taken with a Scanning Electron Microscope (SEM) of the worn areas, especially the dedendum part. Abrasion traces and lines, adhesive wear, thinning of the dedendum, part ruptures from the surface are shown in Figure 6.2 (a) and (b). According to the SEM results, it is understood that there are parts broken off from the surface in the PA6 gear in the image that is the result of 800 rpm. Since the damage occurred at 800 rpm, the PA6 gear was not operated at 1200 rpm. This type of wear is an adhesive type of wear. As the speed increased from 400 rpm to 800 rpm, part ruptures from the dedendum were observed with increasing temperature. PA6 gear has an average temperature of 97.6°C after $10x10^5$ cycles at 800 rpm. This result is shown in Figure 6.15 in the thermal results section. The area that is exposed to the most stress is the dedendum, that is, the part of the tooth root.

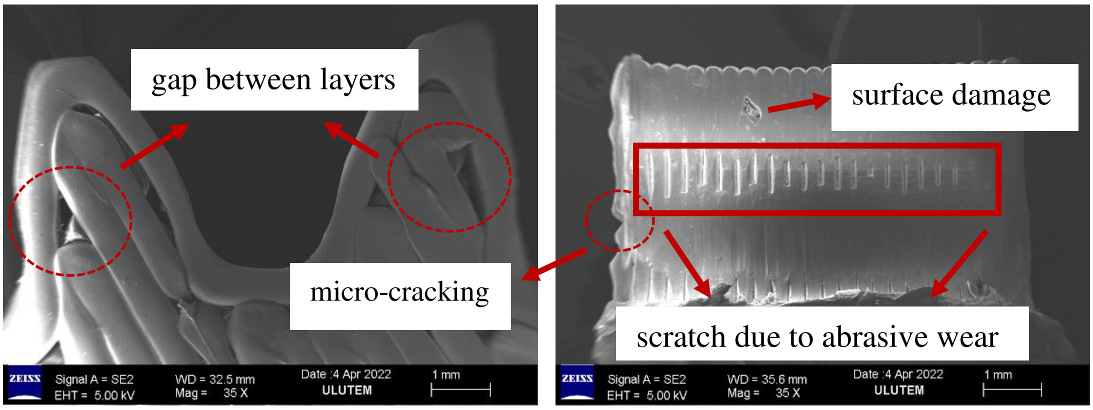

(c) (d)

Figure 6.3 SEM images of Ultem 1010 gear (x35); (c) at 400 rpm, (d) at 800 rpm

Small gaps between the layers of the Ultem 1010 spur gear can be seen in Figure 6.3 (c). Its layered structure is one of the factors preventing heating. When the SEM image of the gear is examined at 800 rpm, vertical lines are seen on the surface. This type of wear is abrasive wear. Vertical wear marks on the Ultem 1010 gear occurred in the addendum region. Since the damage occurred at 800 rpm, the Ultem 1010 gear was not operated at 1200 rpm. An example of this type of wear was reported by Ye.Zhang et al.(Y. Zhang et al., 2020) It has also been seen on the 3D printed Nylon 618 gear, which has worked at 100 rpm. It is shown that Figure 6.4.

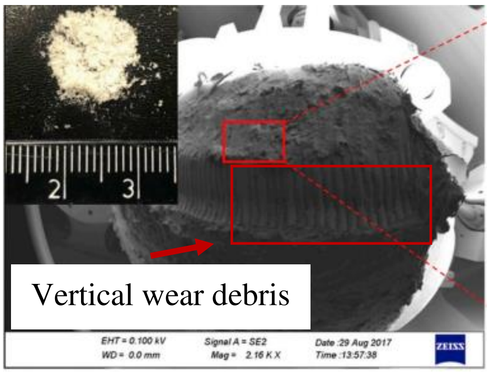

Figure 6.4 SEM image of 3D printed gear Nylon 618 - vertical wear debris(Y. Zhang et al., 2020)

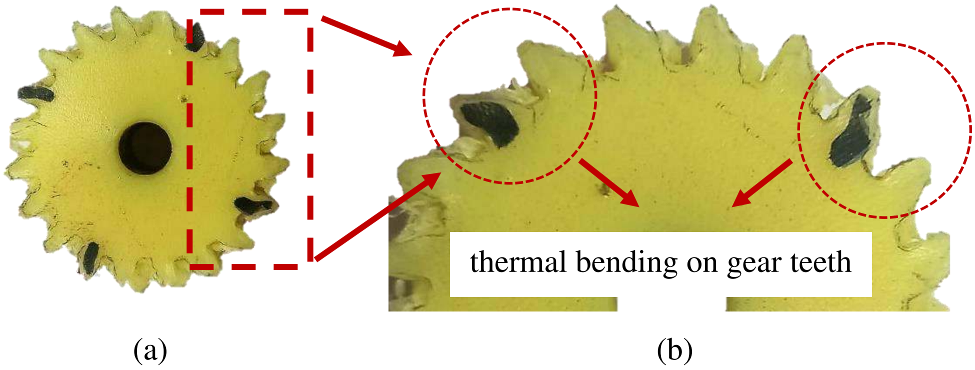

Figure 6.5 (a) PA6 gear working at 800 rpm-10.69 Nm torque, (b) thermal damage and bending of teeth

Another step of the experiments was to run the PA6 and Ultem 1010 gears against the steel gear at 10 Nm, 12 Nm and 15 Nm torque values and at 800 rpm. The torque value of 10 Nm could not be kept constant. Because these gears caused more damage to the PA6 gear, which has a low glass transition temperature, with the increase in temperature as a result of the increase in torque value. As can be seen from Figure 6.5 (a) in the PA6 gear, thermal damage was observed in the teeth, especially with the increase in temperature, the teeth began to soften and thermal bending occurred, Figure 6.5 (b). PA6 gear completed $28x10^3$ cycles (35 minutes) at 800 rpm and 10.69 Nm torque and reached an average temperature of 82°C in this process. In a similar study, the nylon gear was damaged in the torque range of 10 Nm-11Nm for 30 minutes. It is shown in Figure 6.6 .

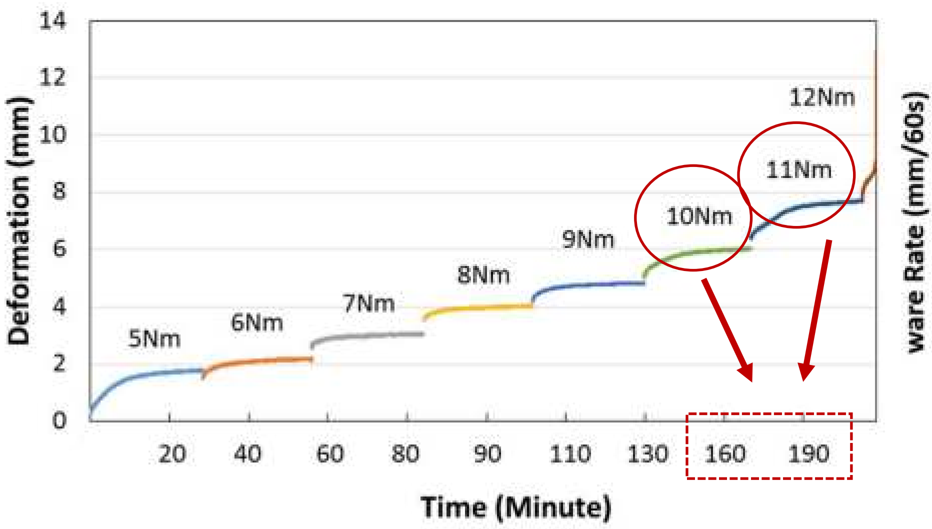

Figure 6.6 Step load test of Nylon gear (Y. Zhang et al., 2020)

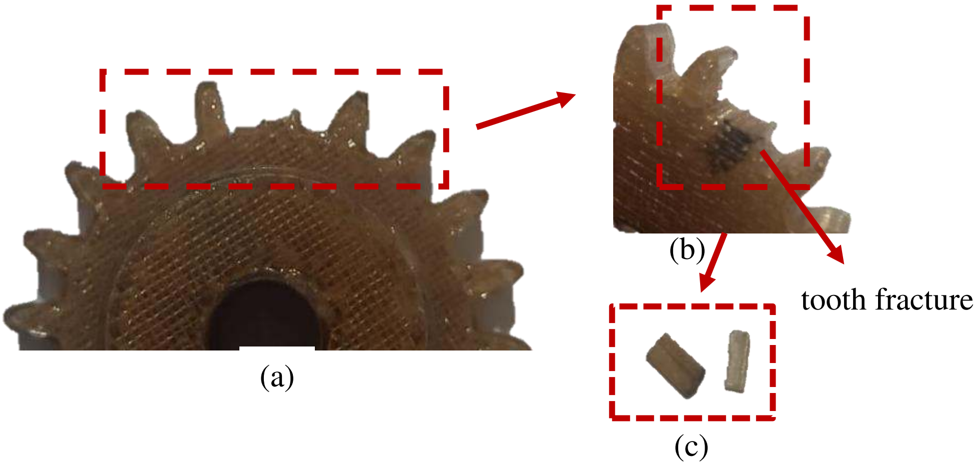

Figure 6.7 (a) Ultem 1010 gear at 800 rpm - 10.17 Nm torque, (b) Gear damage, breakage, (c) broken tooth fragments

Ultem 1010 gear is more brittle when it is produced by 3D printing and is more brittle when exposed to high forces than PA6 gear due to its material structure. Ultem 1010 gear has completed $15.2x10^3$ cycles at 800 rpm and 10.17 Nm torque. As a result, fractures occurred in the tooth roots, as shown in Figure 6.7.

Adis J. Muminovic et al.(Muminović et al., 2023) they produced PLA gears with 20%, 40%, 60%, 80% and 100% filling rates by 3D printing and operated them at 2.4 Nm torque and 1200 rpm. In PLA gears produced with 60%, 80% and 100% infill rate in these gears, fractures in tooth roots and melting on tooth surfaces due to temperature were observed. The working time of these gears is shown in the Figure 6.8. No regional melting was observed on the surface of the Ultem 1010 gear due to the temperature. Only fractures were observed in the tooth root and pitch parts.

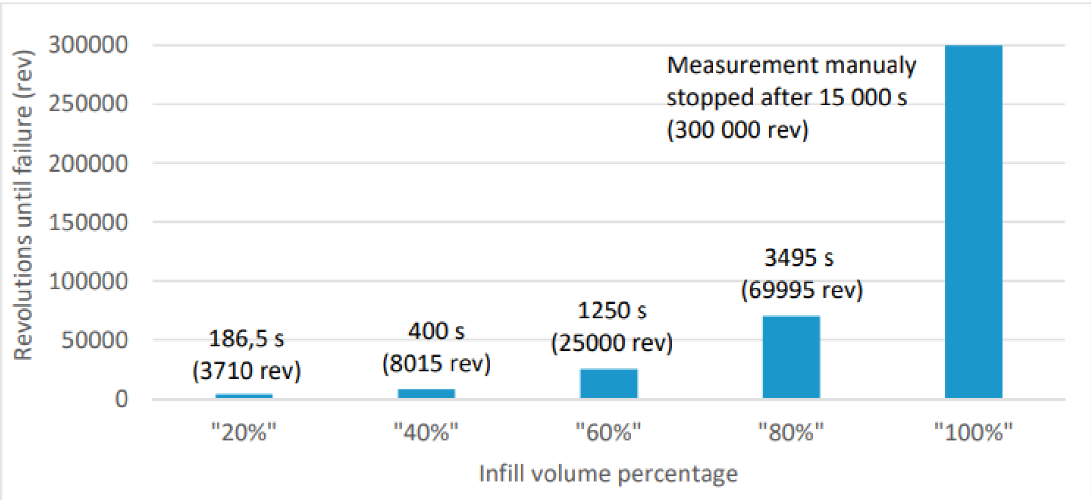

Figure 6.8 Summary results of fatigue life of gears made of PLA with infill (Muminović et al., 2023)

6.3 Surface Roughness Results

Surface roughness is a measurement that describes the smoothness and irregularity of a surface. Surface roughness measurement is used to determine surface irregularities as a result of machine, machining or natural effects. The parameters used to evaluate the surface roughness are Ra and Rz. Ra (Roughness mean value) is a widely accepted and internationally used roughness parameter. It is the arithmetic mean of the absolute values of the roughness profile distances of the midline of the measurement length.

Table 6.3 The Ra averages of the PA6 and Ultem 1010 gears are shown

Working cycle (rpm)	Ra (µm)	
	PA6	Ultem 1010
400	1,16	34,57
800	0,97	21,55
1200	0,92	16,47

Table 6.3 shows the Ra values of the gear pairs. Common roughness behavior in PA6 and Ultem 1010 gear pairs; As the working cycle increases, the surface roughness decreases.

At higher speeds, lower surface roughness is achieved for both materials. However, the surface roughness of ULTEM 1010 gears is higher compared to PA6. This is due to differences in material properties and production methods. Ra results of these gear pairs at 400 rpm, 800 rpm and 1200 rpm are shown in the figures below.

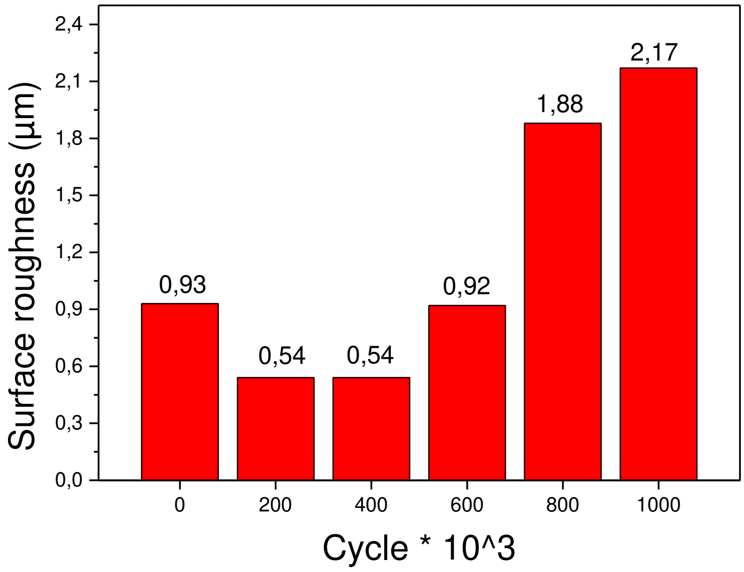

Figure 6.9 Ra values of the PA6 gear at 400 rpm

The Ra values of PA6 and Ultem 1010 gear pairs are shown in Figure 6.9 and Figure 6.10. An increase was observed in the PA6 gear. The Ra values of the Ultem 1010 gear are seen to be high, but the results are gradually decreasing. The reason for these values to be different is due to the different production meters. Since Ultem 1010 is produced in a layered manner, its roughness values are higher than PA6.

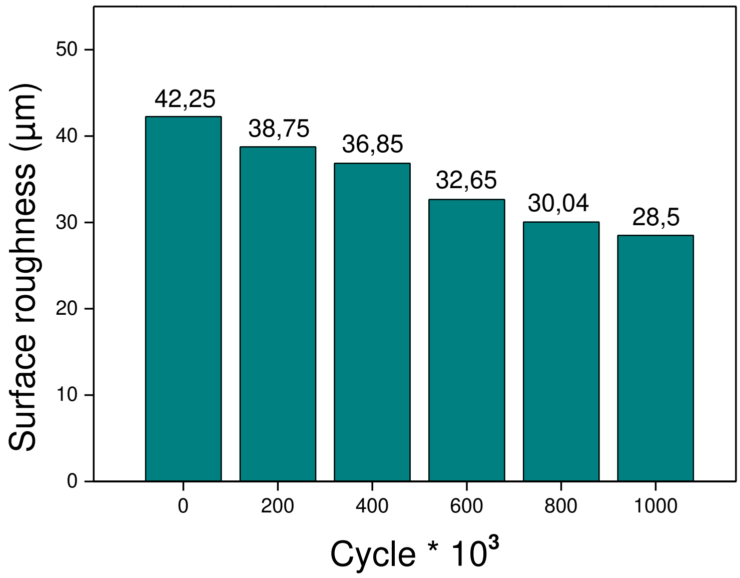

Figure 6.10 Ra values of the Ultem 1010 gear at 400 rpm

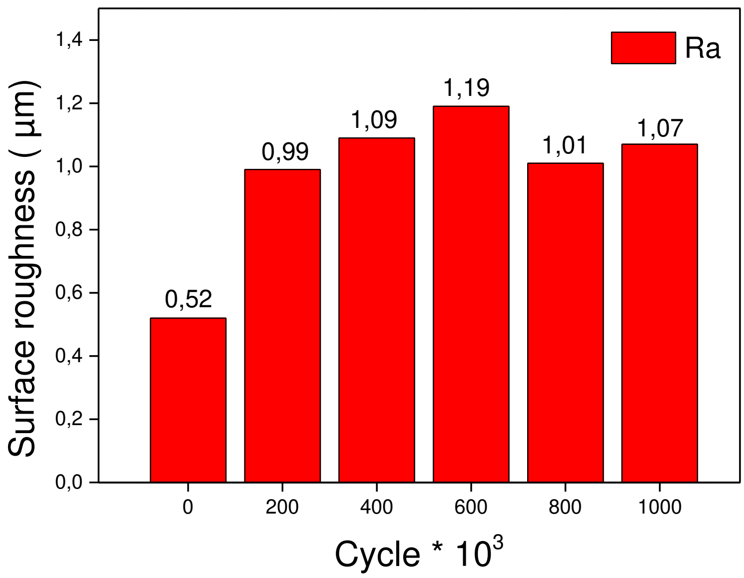

Figure 6.11 Ra values of the PA6 gear at 800 rpm

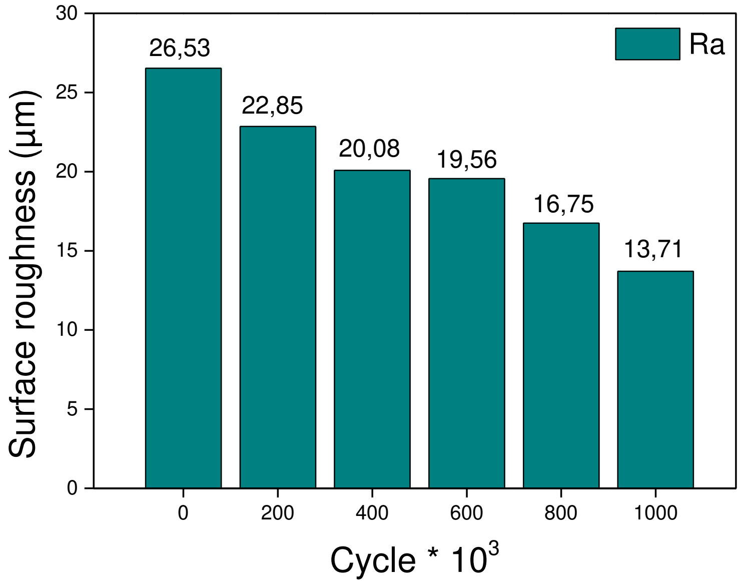

Figure 6.12 Ra values of the Ultem 1010 gear at 800 rpm

A decreasing trend is always seen in the Ultem 1010 gear at 800 rpm and 1200 rpm. Ra values at 1200 rpm are lower than the results at 400 rpm (Figure 6.14). It is concluded that the surface of the Ultem 1010 gear becomes smoother as the speed increases. Since the PA6 gear is produced by machining, its surface is in a better condition than the Ultem 1010 gear, so the Ra results are closer to each other.

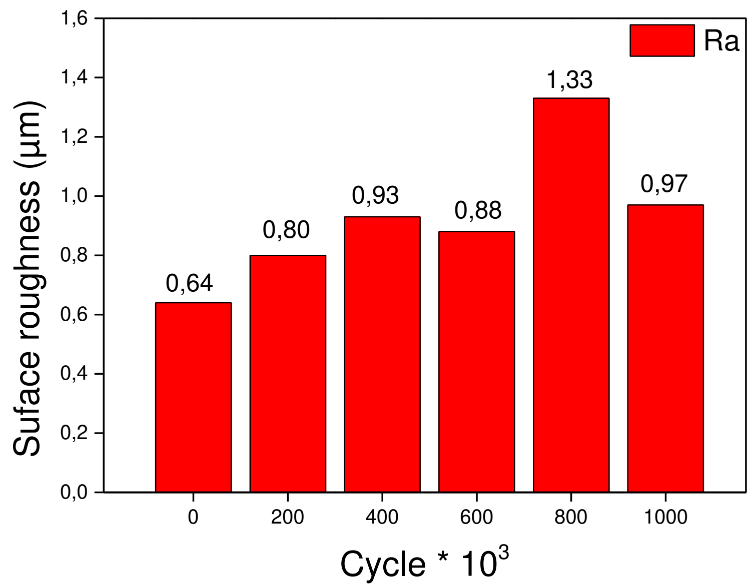

Figure 6.13 Ra values of the PA6 gear at 1200 rpm

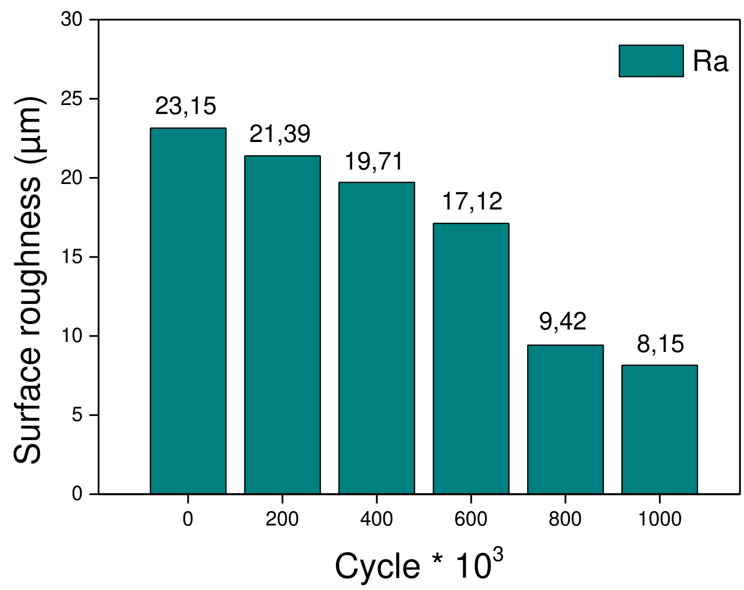

Figure 6.14 Ra values of the Ultem 1010 gear at 1200 rpm

6.4 Thermal Results

Temperature changes and working cycles that gears are exposed to in working environments are among the important factors affecting the wear process. Tests and analyzes performed on gears made of polymer materials such as PA6 and Ultem 1010 should refer to Figure 6.15 to understand the effect of temperature and rotational speed on the wear behavior of gears.

It is seen in Figure 6.15 that the operating temperatures of the PA6 gears increase as the speed increases. Considering that the teeth will generate more friction and heat at high speeds, it can be said that this temperature increase is normal. This affects the amount of friction and wear.

PA6 gear reached a minimum temperature of 87.73°C and a maximum temperature of 103.61°C. that is, an increase of 16-17°C was observed in the PA6 gear. These temperature values were noted at every 200.00 cycles and the average values of the result of 1000.000 cycles were taken into account.

The operating temperature of the Ultem 1010 gear is lower than the PA6 gears. Thermal stability and better mechanical properties of the Ultem 1010 gear are a factor in its better temperature performance.

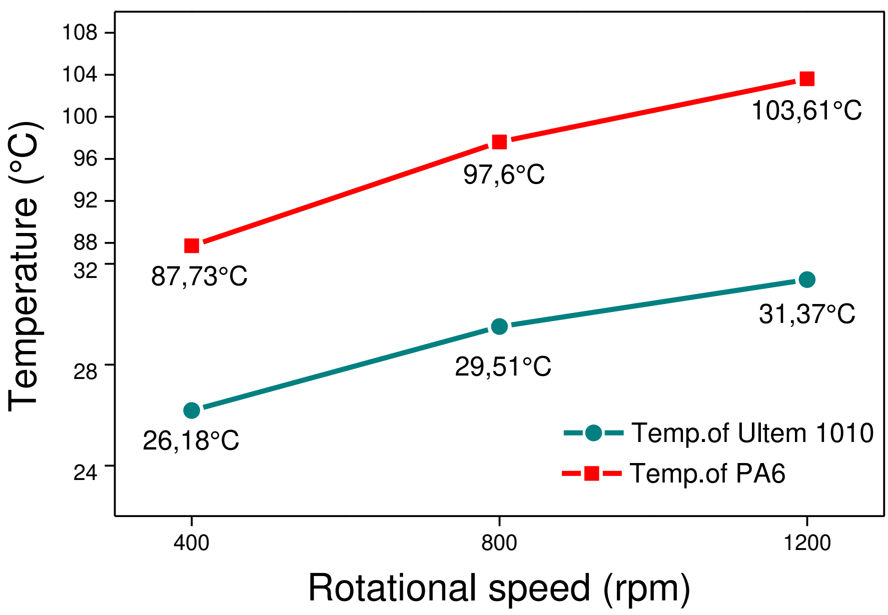

Figure 6.15 Temperature&Rotational speed relationship of gears pairs

PA6 and Ultem 1010 have different responses to temperature due to material chemistry. The glass transition temperature of the PA6 gear, Tg, is 45-65°C. In the experiments carried out, the PA6 gear reached a temperature in the range of 87.73-103.61°C. The temperature value has risen above the glass transition temperature. This affects the chemical structure and durability of the material.

The glass transition temperature of the Ultem 1010 gear is 215°C. It worked in the temperature range of 26.18-31.37°C in the tests. Since this result is below the glass transition temperature, there is no change in its chemical structure.

The thermal conductivity coefficient of the material is an important property. Thermal conductivity coefficient; It expresses how much a material transmits heat depending on its physical or chemical structure. The type of material, the cross-sectional area, the temperature difference between the ends where the heat passes, and the material thickness affect the heat transfer.

The smaller the coefficient of thermal conductivity, the less the material conducts heat. The thermal conductivity coefficients are AISI 1040 51.9 W/mK- PA6 0.25 W/mK

(Ha et al., 2015) and Ultem 1010 0.0644 W/mK. It has been proven that these coefficients and the obtained temperature values evacuate the PEI material from the tooth body even when subjected to long-term operation.

The temperature-torque relationship is shown in Figure 6.16 . The torque value was tried to be kept constant in the range of 3±0.5Nm and it was predicted to work in this range, but the predicted torque value could not be kept exactly constant because the PA6 gear showed excessive wear at high speeds. As torque levels increase in PA6 gears, so does the temperature. This causes the amount of friction and wear to increase and therefore the torque values to increase. In ULTEM 1010 gears, the torque levels are lower compared to PA6. However, the temperature is also at lower levels. This resulted in lower torque values as the thermal properties of the ULTEM 1010 resulted in lower friction and wear.

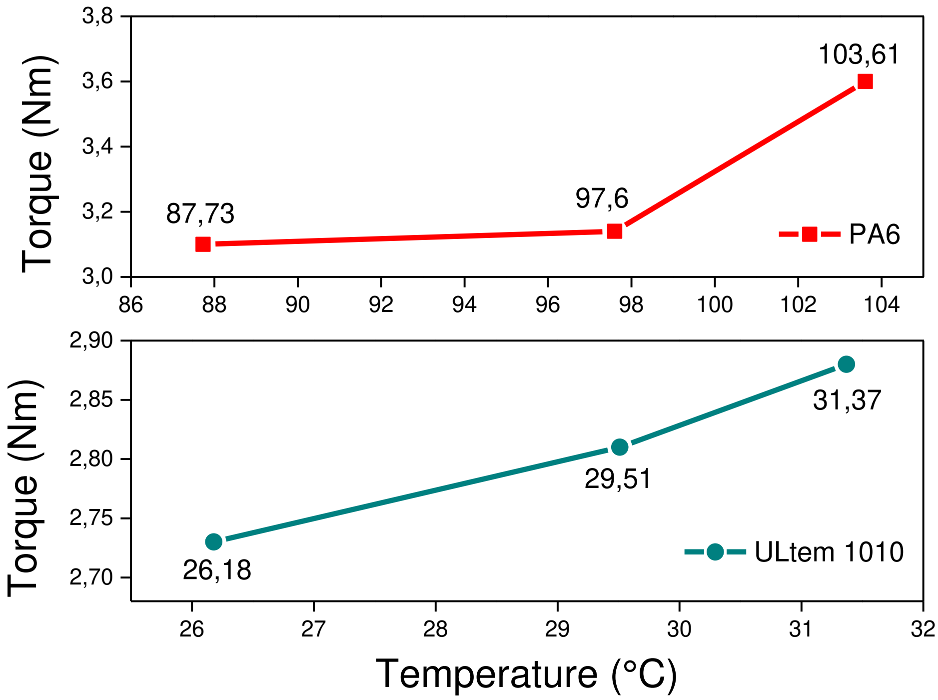

Figure 6.16 The torque&temperature relationship of the gear pairs is shown.

6.5 Noise Results

The noise values of the gear pairs were measured during the gear wear tests. Factors such as the hardness of the material used, whether it is flexible, thermal stability or friction coefficient affect the noise intensity during operation. It is seen that the noise levels of PA6 gears are higher than Ultem 1010 (PEI) gears (Figure 6.17 and Figure 6.18). Also, an increase in the noise levels of the PA6 gears is observed at higher speeds (800 rpm and 1200 rpm) starting from 400 rpm.

The temperature-noise relationship of the PA6 gear is shown in Figure 6.17. The noise values of the PA6 gear, which generates more heat as it works, also increase. The Ultem 1010 gear is a high-performance polymer material. It can also offer lower noise levels compared to PA6 as it has better mechanical properties and thermal stability.

The point to be considered here is the coefficient of friction. The friction coefficient of the Ultem 1010 gear is 0.30, while the friction coefficient of the PA6 gear is 0.82. The Ultem 1010, which has a lower friction coefficient, will generally produce less friction and lower noise due to friction. levels tend to provide.

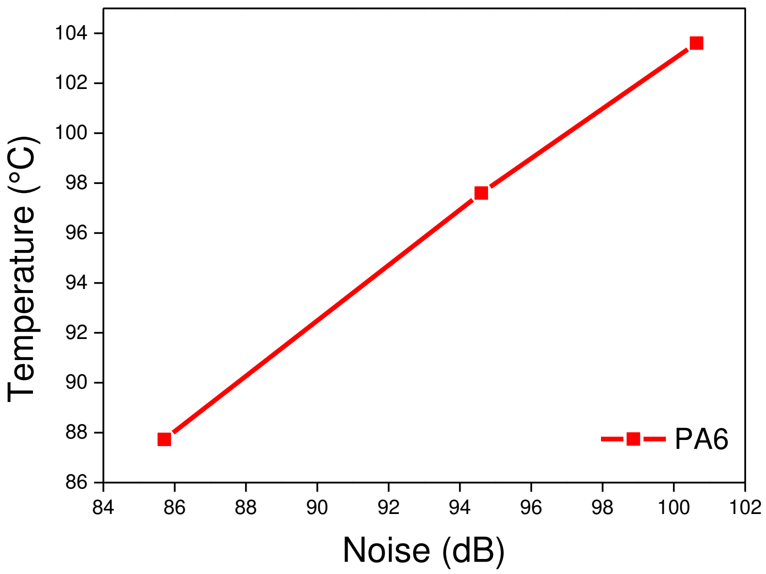

Figure 6.17 Temperature and noise relationship of PA6 gear

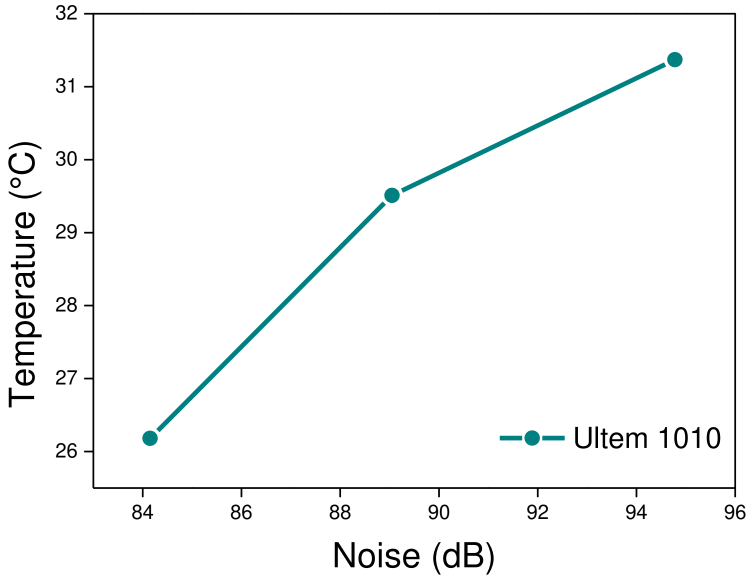

Figure 6.18 Temperature and noise relationship of Ultem 1010 gear

Figure 6.18 shows the noise-temperature relationship of the Ultem gear. While the noise values are 84.15 dB at 26.18°C, they reach 94.78 dB at 31.37°C. Parts produced with 3D printing usually have higher surface roughness. Ultem1010 Ra values are shown in Table 6.2 . Rough surfaces increase the friction between the teeth and increase the noise level. Therefore, the noise values are close with the PA6 gear. The noise values of the Ultem 1010 in Figure 6.18 are between 84 dB and 96 dB. However, when looking at Figure 6.17, PA6 noise values are between 85 dB and 102 dB. Although there was not much difference, the Ultem 1010 worked silently according to the noise results. Although the Ultem 1010 gave a better result in terms of noise results performance, the results were close to each other. Another factor here is the layer thickness of the Ultem 1010 gear. A thinner layer thickness can result in lower surface roughness and a smoother surface, which can reduce noise levels, but also reduce production efficiency. The Ultem 1010 gear has a layer thickness of 330 μm.

CHAPTER 7
CONCLUSION

In this thesis, the wear behavior of the plastic gears used was investigated. Basically, the wear behavior of the PEI gear was taken into account and it was taken into account whether it would be preferred instead of the PA6 gear. The PA6 gear is a frequently used gear in the industry. All tests were carried out under the same conditions in the same environment.

The results of the study are shared as follows;

- The PA6 gear has reached very high temperature values as a result of the tests. The temperature values of the PEI gear are quite low. The heated material softens and wears more, and its life is reduced.

- As a result of the tests, the PA6 gear performed better at low and medium speeds, and the amount of wear was less than the Ultem gear. However, the Ultem 1010 gear performs better at high speeds and is less worn than the PA6 gear.

- In terms of roughness, the surface of the Ultem 1010 gear has become more and more smooth compared to the starting point. This behavior was also seen in the PA6 gear, but because the PA6 gear is produced in a smoother way than the ULTEM 1010 gear. There is no noticeable big difference in the PA6 gear.

- For PA6 gear; As the speed increases, the amount of wear also increases, and for the ULTEM 1010 gear, this is the opposite, the amount of wear showed a decreasing trend as the speed increases.

REFERENCES

Aleksandar Vencl, Vlada Gašić, & Blaža Stojanović. (n.d.). *Fault tree analysis of most common rolling bearing tribological failures*.

Amiri, M., & Khonsari M., M. (2010). On the Thermodynamics of Friction and Wear―A Review _ Enhanced Reader. *Entropy*. chrome-extension://dagcmkpagjlhakfdhnbomgmjdpkdklff/enhanced-reader.html?pdf=https%3A%2F%2Fbrxt.mendeley.com%2Fdocument%2Fcontent%2F9a8d1ce3-13e7-3b93-8dc5-3ee834c4dc51

Amirruddin, M. S., Ismail, K. I., & Yap, T. C. (2021). Effect of layer thickness and raster angle on the tribological behavior of 3D printed materials. *Materials Today: Proceedings*, *48*, 1821–1825. https://doi.org/10.1016/j.matpr.2021.09.139

Asi, O. (2006). Fatigue failure of a helical gear in a gearbox. *Engineering Failure Analysis*, *13*(7), 1116–1125. https://doi.org/10.1016/j.engfailanal.2005.07.020

ASM International. Handbook Committee. (n.d.). *ASM handbook*.

Blau, P. J., & Budinski, K. G. (n.d.). Development and use of ASTM standards for wear testing 1. In *Wear*.

Breedsa, A. R., Kukureka, S. N., Maob, K., Waltonb, D., & Hookeb, C. J. (1993). Wear behaviour of acetal gear pairs. In *Wear* (Vol. 166).

Briscoe, Y. B. J., & Tabor, D. (n.d.). *Friction and Adhesion Surface Forces in Friction and Adhesion*.

BUCKLEY, H. D. (n.d.). *Surface Effects in Adhesion, Friction, Wear, and Lubrication*.

Chaudhari, M., Jogi, B. F., & Pawade, R. S. (2018). Comparative Study of Part Characteristics Built Using Additive Manufacturing (FDM). *Procedia Manufacturing*, *20*, 73–78. https://doi.org/10.1016/j.promfg.2018.02.010

Chockalingam, K., Jawahar, N., & Chandrasekhar, U. (2006). Influence of layer thickness on mechanical properties in stereolithography. *Rapid Prototyping Journal*, *12*(2), 106–113. https://doi.org/10.1108/13552540610652456

Dearn, K. D., Hoskins, T. J., Petrov, D. G., Reynolds, S. C., & Banks, R. (2013). Applications of dry film lubricants for polymer gears. *Wear*, *298–299*(1), 99–108. https://doi.org/10.1016/j.wear.2012.11.003

Dhanasekaran, S., & Gnanamoorthy, R. (2008a). Gear tooth wear in sintered spur gears under dry running conditions. *Wear*, *265*(1–2), 81–87. https://doi.org/10.1016/j.wear.2007.08.025

Dhanasekaran, S., & Gnanamoorthy, R. (2008b). Gear tooth wear in sintered spur gears under dry running conditions. *Wear*, *265*(1–2), 81–87. https://doi.org/10.1016/j.wear.2007.08.025

Düzcükoglu Hayrettin, R. Y. , E. U. (2010). Enhanced Reader. *Journal Of Failure Analysis and Preventation*, 545–555.

Ebersbach, S., Peng, Z., & Kessissoglou, N. J. (2006). The investigation of the condition and faults of a spur gearbox using vibration and wear debris analysis techniques. *Wear*, *260*(1–2), 16–24. https://doi.org/10.1016/j.wear.2004.12.028

Errichello, R. (2002). How to analyze gear failures. *Journal of Failure Analysis and Prevention*, *2*(6), 8–16. https://doi.org/10.1007/bf02715492

Fernandes, P. J. L. (1996). TOOTH BENDING FATIGUE FAILURES IN GEARS. In *Engineering Failure Analysis* (Vol. 3, Issue 3).

Finkin, E. F. (n.d.). *Adhesive wear: a general review of the state of experimental knowledge and theory*.

Flodin, A. (n.d.). *Wear Investigation of Spur Gear Teeth*.

Fontalvo, G. A., Humer, R., Mitterer, C., Sammt, K., & Schemmel, I. (2006). Microstructural aspects determining the adhesive wear of tool steels. *Wear*, *260*(9–10), 1028–1034. https://doi.org/10.1016/j.wear.2005.07.001

Fouly, A., Assaifan, A. K., Alnaser, I. A., Hussein, O. A., & Abdo, H. S. (2022). Evaluating the Mechanical and Tribological Properties of 3D Printed Polylactic-Acid (PLA) Green-Composite for Artificial Implant: Hip Joint Case Study. *Polymers*, *14*(23). https://doi.org/10.3390/polym14235299

Geitner, F. K. (n.d.). *Adhesive Wear Metallurgical Failure Analysis Adhesive Wear Mechanisms of tool wear*.

Glodež, S., Winter, H., & Stüwe, H. P. (1997). A fracture mechanics model for the wear of gear flanks by pitting. In *Wear* (Vol. 208).

Gordelier, T. J., Thies, P. R., Turner, L., & Johanning, L. (2019). Optimising the FDM additive manufacturing process to achieve maximum tensile strength: a state-of-the-art review. In *Rapid Prototyping Journal* (Vol. 25, Issue 6, pp. 953–971). Emerald Group Holdings Ltd. https://doi.org/10.1108/RPJ-07-2018-0183

Gurunathan, C., Kirupasankar, S., & Gnanamoorthy, R. (2011). Wear characteristics of polyamide nanocomposite spur gears. *Proceedings of the Institution of Mechanical Engineers, Part J: Journal of Engineering Tribology*, *225*(5), 299–306. https://doi.org/10.1177/1350650111401282

Ha, S. M., Kwon, O. H., Oh, Y. G., Kim, Y. S., Lee, S. G., Won, J. C., Cho, K. S., Kim, B. G., & Yoo, Y. (2015). Thermally conductive polyamide 6/carbon filler composites based on a hybrid filler system. *Science and Technology of Advanced Materials*, *16*(6). https://doi.org/10.1088/1468-6996/16/6/065001

Han, P., Tofangchi, A., Deshpande, A., Zhang, S., & Hsu, K. (2019a). *An approach to improve interface healing in FFF-3D printed Ultem 1010 using laser pre-deposition heating*. *34*, 672–677. https://doi.org/10.1016/j.promfg.2019.06.195

Han, P., Tofangchi, A., Deshpande, A., Zhang, S., & Hsu, K. (2019b). *An approach to improve interface healing in FFF-3D printed Ultem 1010 using laser pre-deposition heating*. *34*, 672–677. https://doi.org/10.1016/j.promfg.2019.06.195

Harsha, K. M., Seetharama Rao, Y., & Jagannadha rao, D. (2021). Comparison of wear behaviour of polymer spur gears using FDM process. *IOP Conference Series: Materials Science and Engineering*, *1168*(1), 012028. https://doi.org/10.1088/1757-899x/1168/1/012028

HONG, W., CAI, W., WANG, S., & TOMOVIC, M. M. (2018). Mechanical wear debris feature, detection, and diagnosis: A review. In *Chinese Journal of Aeronautics* (Vol. 31, Issue 5, pp. 867–882). Chinese Journal of Aeronautics. https://doi.org/10.1016/j.cja.2017.11.016

Hsu, S. M., & Klaus, E. E. (1978). Estimation of the molecular junction temperatures in four-ball contacts by chemical reaction rate studies. *ASLE Transactions*, *21*(3), 201–210. https://doi.org/10.1080/05698197808982875

Huang, J., Qin, Q., & Wang, J. (2020). A review of stereolithography: Processes and systems. In *Processes* (Vol. 8, Issue 9). MDPI AG. https://doi.org/10.3390/PR8091138

Imrek, H. (2009). Performance improvement method for Nylon 6 spur gears. *Tribology International*, *42*(3), 503–510. https://doi.org/10.1016/j.triboint.2008.08.011

Jiang, S., Liao, G., Xu, D., Liu, F., Li, W., Cheng, Y., Li, Z., & Xu, G. (2019). Mechanical properties analysis of polyetherimide parts fabricated by fused deposition modeling. *High Performance Polymers*, *31*(1), 97–106. https://doi.org/10.1177/0954008317752822

Johnson, K. L. (1989). The strength of surfaces in rolling contact. *Proceedings of the Institution of Mechanical Engineers, Part C: Journal of Mechanical Engineering Science*, *203*(3), 151–163. https://doi.org/10.1243/PIME_PROC_1989_203_100_02

Jun, G., Lee, J. W., Shin, Y., Kim, K., & Hwang, W. (2020). Solvent-aided direct adhesion of a metal/polymer joint using micro/nano hierarchical structures. *Journal of Materials Processing Technology*, *285*. https://doi.org/10.1016/j.jmatprotec.2020.116744

K D Dearn*, & D Walto. (n.d.). *World Congress on Engineering 2009. Volume 2.*

Kandeva, M., Vencl, A., & Karastoyanov, D. (2016). *Advanced Tribological Coatings for Heavy-Duty Applications: Case Studies "Creation of a flexible methodology for development and management of innovative projects in scientific organizations" View project TECHNOLOGICAL FEATURES AND REGULARITIES OF CREATION OF NEW HIGH WEAR RESISTANT COMPOSITE COATINGS ON TITANIUM ALLOYS BY ELECTRICAL SPARK DEPOSITION PROCESS View project*. https://www.researchgate.net/publication/313165229

Kato, K. (2000). Wear in relation to friction-a review. In *Wear*. www.elsevier.comrlocaterwear

Kaur, G., & Pavia, S. (2020). Physical properties and microstructure of plastic aggregate mortars made with acrylonitrile-butadiene-styrene (ABS), polycarbonate (PC), polyoxymethylene (POM) and ABS/PC blend waste. *Journal of Building Engineering*, *31*. https://doi.org/10.1016/j.jobe.2020.101341

Kechagias, J. D., & Maropoulos, S. (2015a). *An Investigation of Sloped Surface Roughness of Direct Poly-Jet 3D Printing Machinabiity of PA 66-GF 30 View project Filament Material Extrusion 3D printing process optimization View project*. https://www.researchgate.net/publication/282847491

Kechagias, J. D., & Maropoulos, S. (2015b). *An Investigation of Sloped Surface Roughness of Direct Poly-Jet 3D Printing Machinabiity of PA 66-GF 30 View project Filament Material Extrusion 3D printing process optimization View project*. https://www.researchgate.net/publication/282847491

Klaus, E. E., & Bieber, H. E. (1964). Effect of some physical and chemical properties of lubricants on boundary lubrication. *ASLE Transactions*, *7*(1), 1–10. https://doi.org/10.1080/05698196408972030

Klosterman, D., Chartoff, R., Graves, G., Osborne, N., & Priore, B. (n.d.). *Interfacial characteristics of composites fabricated by laminated object manufacturing*. www.udri.udayton.edu/rpdl

Kumar, S., Choudhary, A. K. S., Kishore, A., Amit, S., Gupta, K., & Student, U. G. (2016). A Comparison of Additive Manufacturing Technologies. *IJIRST-*

International Journal for Innovative Research in Science & Technology|, *3*. www.ijirst.org

Liu, H., Liu, H., Zhu, C., & Tang, J. (2020). Study on gear contact fatigue failure competition mechanism considering tooth wear evolution. *Tribology International*, *147*. https://doi.org/10.1016/j.triboint.2020.106277

Liu, H., & Zhu, C. (n.d.). */ Mechanism and Machine Theory 145 (2020) 103701 Fig. 1. Gear lubrication in engineering practices* (Vol. 10).

Lu, H., Lee, Y. K., Oguri, M., & Powers, J. M. (2006). Properties of a dental resin composite with a spherical inorganic filler. *Operative Dentistry*, *31*(6), 734–740. https://doi.org/10.2341/05-154

Manapat, J. Z., Chen, Q., Ye, P., & Advincula, R. C. (2017). 3D Printing of Polymer Nanocomposites via Stereolithography. In *Macromolecular Materials and Engineering* (Vol. 302, Issue 9). Wiley-VCH Verlag. https://doi.org/10.1002/mame.201600553

Mantrala, M. K., Suresh, G., Narayana, K. L., & Mallik, M. K. (2017). A Review on Development of Medical Implants by Rapid Prototyping Technology Article in. *International Journal of Pure and Applied Mathematics*, *117*(21), 257–276.

Mao, K., Greenwood, D., Ramakrishnan, R., Goodship, V., Shrouti, C., Chetwynd, D., & Langlois+, P. (2019). The wear resistance improvement of fibre reinforced polymer composite gears. *Wear*, *426–427*, 1033–1039. https://doi.org/10.1016/j.wear.2018.12.043

Mao, K., Li, W., Hooke, C. J., & Walton, D. (2009). Friction and wear behaviour of acetal and nylon gears. *Wear*, *267*(1–4), 639–645. https://doi.org/10.1016/j.wear.2008.10.005

Mao, K., Li, W., Hooke, C. J., & Walton, D. (2010). Polymer gear surface thermal wear and its performance prediction. *Tribology International*, *43*(1–2), 433–439. https://doi.org/10.1016/j.triboint.2009.07.006

Mcdonald, A., & Stott, F. (1987). *EFFECT OF TEMPERATURE ON THE CORROSIVE WEAR OF CAST-IRON IN OIL-SULPHURIC ACID ENVIRONMENTS* (Vol. 4).

Mishina, H., & Hase, A. (2013). Wear equation for adhesive wear established through elementary process of wear. *Wear*, *308*(1–2), 186–192. https://doi.org/10.1016/j.wear.2013.06.016

Mishina, R. A. H. (1981). *Susumu Norose The Behawior of Adhered Fragments Interposed Between Sliding Surfaces and the Formation Process of Wear Particles*. http://tribology.asmedigitalcollection.asme.org/pdfaccess.ashx?url=/data/journals/jotre9/28641/

Mokhtar, A., Zaki, M., & A Shawki, G. S. (1980). Printed in the Netherlands CORRELATION BETWEEN THE FRICTIONAL BEHAVIOUR AND THE PHYSICAL PROPERTIES OF METALS. In *Wear* (Vol. 65). Elsevier Sequoia S.A.

Molinari, J. F., Aghababaei, R., Brink, T., Frérot, L., & Milanese, E. (2018a). Adhesive wear mechanisms uncovered by atomistic simulations. In *Friction* (Vol. 6, Issue 3, pp. 245–259). Tsinghua University Press. https://doi.org/10.1007/s40544-018-0234-6

Molinari, J. F., Aghababaei, R., Brink, T., Frérot, L., & Milanese, E. (2018b). Adhesive wear mechanisms uncovered by atomistic simulations. In *Friction* (Vol. 6, Issue 3, pp. 245–259). Tsinghua University Press. https://doi.org/10.1007/s40544-018-0234-6

Monzón, M. D., Ortega, Z., Martínez, A., & Ortega, F. (2015). Standardization in additive manufacturing: activities carried out by international organizations and projects. In *International Journal of Advanced Manufacturing Technology* (Vol. 76, Issues 5–8, pp. 1111–1121). Springer London. https://doi.org/10.1007/s00170-014-6334-1

MOORE. A. MARTIN. (1978). *Abrasive wear*.

Muminović, A. J., Braut, S., Božić, Ž., Pervan, N., & Skoblar, A. (2023). Experimental failure analysis of polylactic acid gears made by additive manufacturing. *Procedia Structural Integrity*, *46*, 125–130. https://doi.org/10.1016/j.prostr.2023.06.021

Muminovic, A. J., Pervan, N., Delic, M., Muratovic, E., Mesic, E., & Braut, S. (2022). Failure analysis of nylon gears made by additive manufacturing. *Engineering Failure Analysis*, *137*. https://doi.org/10.1016/j.engfailanal.2022.106272

Nuruzzaman, D. M., Chowdhury, M. A., & Rahaman, M. L. (2011). Effect of duration of rubbing and normal load on friction coefficient for polymer and composite materials. *Industrial Lubrication and Tribology*, *63*(5), 320–326. https://doi.org/10.1108/00368791111154931

Olivera, S., Muralidhara, H. B., Venkatesh, K., Gopalakrishna, K., & Vivek, C. S. (2016). Plating on acrylonitrile–butadiene–styrene (ABS) plastic: a review. In *Journal of Materials Science* (Vol. 51, Issue 8, pp. 3657–3674). Springer New York LLC. https://doi.org/10.1007/s10853-015-9668-7

Pagac, M., Hajnys, J., Ma, Q. P., Jancar, L., Jansa, J., Stefek, P., & Mesicek, J. (2021). A review of vat photopolymerization technology: Materials, applications, challenges, and future trends of 3d printing. In *Polymers* (Vol. 13, Issue 4, pp. 1–20). MDPI AG. https://doi.org/10.3390/polym13040598

Parandoush, P., & Lin, D. (2017). A review on additive manufacturing of polymer-fiber composites. In *Composite Structures* (Vol. 182, pp. 36–53). Elsevier Ltd. https://doi.org/10.1016/j.compstruct.2017.08.088

Patil, C., Shrigandhi, G., Karad, V., Girase, S. B., Patil, C. K., Shisode, S. P., & Shrigandhi, G. D. (n.d.). Failure Analysis of Drive Shaft View project Modal Analysis of High Pressure Fuel Injection Pipe for a DV-10 V Diesel Engine View project WEAR AND FATIGUE ANALYSIS OF EN-19 STEEL. *International Journal for Research in Engineering Application & Management*. https://doi.org/10.18231/2454-9150.2018.1401

Petrica, M., Badisch, E., & Peinsitt, T. (2013). Abrasive wear mechanisms and their relation to rock properties. *Wear*, *308*(1–2), 86–94. https://doi.org/10.1016/j.wear.2013.10.005

Phillips, B. T., Allder, J., Bolan, G., Nagle, R. S., Redington, A., Hellebrekers, T., Borden, J., Pawlenko, N., & Licht, S. (2020). Additive manufacturing aboard a moving vessel at sea using passively stabilized stereolithography (SLA) 3D printing. *Additive Manufacturing*, *31*. https://doi.org/10.1016/j.addma.2019.100969

Podgornik, B. (2020). Adhesive Wear Failures. In *Failure Analysis and Prevention* (pp. 1–20). ASM International. https://doi.org/10.31399/asm.hb.v11.a0006791

Polanec Brigita, Z. F., Bončina Tonica, T. F. , & Glodež Srečko. (2021). Experimental Investigation of the Wear Behaviour of Coated Polymer Gears _ Enhanced Reader. *Polymers*, 1–13. https://doi.org/https://doi.org/10.3390/polym13203588

Rabinowicz, E., Dunn, L. A., & Russell, P. G. (n.d.). *WEAR 345 A STUDY OF ABRASIVE WEAR UNDER THREE-BODY CONDITIONS*.

Raghav, M. S., Singh, A., & Patel, S. (2022). Fault analysis of spur gear using XFEM. *Engineering Failure Analysis*, *134*. https://doi.org/10.1016/j.engfailanal.2022.106060

Rana, V., Jain, N. K., & Pathak, S. (2023). Improving functional performance characteristics of spur gears through flank modifications by non-contact advanced finishing process. *International Journal of Advanced Manufacturing Technology*, *124*(5–6), 1787–1811. https://doi.org/10.1007/s00170-022-10566-9

Reich, M. J., Woern, A. L., Tanikella, N. G., & Pearce, J. M. (2019). Mechanical properties and applications of recycled polycarbonate particle material extrusion-based additive manufacturing. *Materials*, *12*(10). https://doi.org/10.3390/ma12101642

Rivas, J. S., Coronado, J. J., & Gómez, A. L. (2006). Tribological aspects for the shafts and bearings of sugar cane mills. *Wear*, *261*(7–8), 779–784. https://doi.org/10.1016/j.wear.2006.01.026

Roy, R., & Mukhopadhyay, A. (2020). Tribological studies of 3D printed ABS and PLA plastic parts. *Materials Today: Proceedings*, *41*, 856–862. https://doi.org/10.1016/j.matpr.2020.09.235

Rymuza, Z. (2007). Tribology of Polymers. In *ARCHIVES OF CIVIL AND MECHANICAL ENGINEERING: Vol. VII* (Issue 4).

Sargent, L. B. (1978). On the fundamental nature of metal-metal adhesion. *ASLE Transactions*, *21*(4), 285–290. https://doi.org/10.1080/05698197808982886

Sathees Kumar, S., Sridhar Babu, B., Prabhakar, N., & Nithin Chakravarthy, C. (2021). Thermal stress reduction on polyamide gear by finite element method. *Materials Today: Proceedings*, *46*, 819–825. https://doi.org/10.1016/j.matpr.2020.12.799

Scott, J., Gupta, N., Weber, C., & Caffrey, T. (2012). *Additive Manufacturing: Status and Opportunities*.

Senophoe, M., & Yadav, A. (2012). Different types Failure in gears-A Review. In *International Journal of Science, Engineering and Technology Research (IJSETR)* (Vol. 1, Issue 5).

Singh, P. K., Siddhartha, & Singh, A. K. (2018). An investigation on the thermal and wear behavior of polymer based spur gears. *Tribology International*, *118*, 264–272. https://doi.org/10.1016/j.triboint.2017.10.007

Stachıwiak W.Gwidon, & Batchelor W.Andrew. (1993). *TeamLRN*.

Stachowiak, G. W. (Gwidon W.), & Batchelor, A. W. (Andrew W.). (1993a). *Engineering tribology*. Elsevier.

Stachowiak, G. W. (Gwidon W.), & Batchelor, A. W. (Andrew W.). (1993b). *Engineering tribology*. Elsevier.

Sun, W., Giusca, C. L., & Lancaster, A. J. (2017). *Surface texture measurements of gear surfaces using stylus instruments X-ray computed tomography, surface metrology, verification and calibration of instrumentaion, numerical modelling View project MetHPM: Metrology for highly parallel manufacturing View project*. www.npl.co.uk

Szykiedans, K., & Credo, W. (2016). Mechanical properties of FDM and SLA low-cost 3-D prints. *Procedia Engineering*, *136*, 257–262. https://doi.org/10.1016/j.proeng.2016.01.207

Terwey, J. T., Fourati, M. A., Pape, F., & Poll, G. (2020). Energy-based modelling of adhesive wear in the mixed lubrication regime. *Lubricants*, *8*(2). https://doi.org/10.3390/lubricants8020016

Tezel, T., Topal, E. S., & Kovan, V. (2020). Failure analysis of 3D-printed steel gears. *Engineering Failure Analysis*, *110*. https://doi.org/10.1016/j.engfailanal.2020.104411

The adhesion of clean metals. (1956). *Proceedings of the Royal Society of London. Series A. Mathematical and Physical Sciences*, *233*(1195), 429–442. https://doi.org/10.1098/rspa.1956.0001

Tunalioglu, M. S., & Torun, T. (2021). The investigation of wear on three-dimensional printed spur gears. *Proceedings of the Institution of Mechanical Engineers, Part E: Journal of Process Mechanical Engineering*, *235*(6), 2027–2034. https://doi.org/10.1177/09544089211027732

Valino, A. D., Dizon, J. R. C., Espera, A. H., Chen, Q., Messman, J., & Advincula, R. C. (2019). Advances in 3D printing of thermoplastic polymer composites and nanocomposites. In *Progress in Polymer Science* (Vol. 98). Elsevier Ltd. https://doi.org/10.1016/j.progpolymsci.2019.101162

Vidakis, N., Petousis, M., Vaxevanidis, N., & Kechagias, J. (2020). Surface roughness investigation of poly-jet 3D printing. *Mathematics*, *8*(10), 1–14. https://doi.org/10.3390/math8101758

Wagner, M., & Isaacson, A. (2019). *AGMA Technical Paper A Comparison of Surface Roughness Measurement Methods for Gear Tooth Working Surfaces*.

Walton, D., & Goodwin, A. J. (1998). The wear of unlubricated metallic spur gears. In *Wear* (Vol. 222).

Wang, W., Wei, P., Liu, H., Yu, Y., & Zhou, H. (n.d.). *Damage behavior due to rolling contact fatigue and bending fatigue of a gear using crystal plasticity modeling _ Enhanced Reader*.

Wei, X., Zou, N., Zeng, L., & Pei, Z. (2022). PolyJet 3D printing: Predicting color by multilayer perceptron neural network. *Annals of 3D Printed Medicine*, *5*, 100049. https://doi.org/10.1016/j.stlm.2022.100049

Wickramasinghe, S., Do, T., & Tran, P. (2020). FDM-Based 3D printing of polymer and associated composite: A review on mechanical properties, defects and treatments. In *Polymers* (Vol. 12, Issue 7, pp. 1–42). MDPI AG. https://doi.org/10.3390/polym12071529

Wong, K. V., & Hernandez, A. (2012). A Review of Additive Manufacturing. *ISRN Mechanical Engineering*, *2012*, 1–10. https://doi.org/10.5402/2012/208760

Xu, W., Li, C., Zhang, Y., -, al, Pradal, C., Yakubov, G. E., & K Williams, M. A. (n.d.). Friction, lubrication and wear: a survey of work during the last decade You may also like Electrostatic atomization minimum quantity lubrication machining: from mechanism to application Hybrid and electric vehicle tribology: a review Hemanth G, Suresha B and Ananthapadmanabha-Lubrication by biomacromolecules: mechanisms and biomimetic strategies. In *British Journal of Applied Physics REVIEW ARTICLES*.

Yahagi, Y., & Mizutani, Y. (1984). CORROSIVE WEAR OF STEEL IN GASOLINE-ETHANOL-WATER MIXTURES. In *Wear* (Vol. 97).

Yamamoto, T., & Buckley, D. H. (1982). *Wear Mechanism Based on Adhesion*.

Yao, R., Xu, G., Mao, S. S., Yang, H. Y., Sang, X. T., Sun, W., & Mao, Y. L. (2016). Three-dimensional printing: review of application in medicine and hepatic surgery. *Cancer Biology and Medicine*, *13*(4), 443–451. https://doi.org/10.20892/j.issn.2095-3941.2016.0075

Yilmaz, M., Yilmaz, N. F., & Kalkan, M. F. (2022). Rheology, Crystallinity, and Mechanical Investigation of Interlayer Adhesion Strength by Thermal Annealing of Polyetherimide (PEI/ULTEM 1010) Parts Produced by 3D Printing. *Journal* *of Materials Engineering and Performance*. https://doi.org/10.1007/s11665-022-07049-z

Zhang, Y., & Fang, Z. (n.d.). *Analysis of tooth contact and load distribution of helical gears with crossed axes*.

Zhang, Y., Purssell, C., Mao, K., & Leigh, S. (2020). A physical investigation of wear and thermal characteristics of 3D printed nylon spur gears. *Tribology International*, *141*. https://doi.org/10.1016/j.triboint.2019.105953

Zhang, Z. chen, Li, P. lun, Chu, F. ting, & Shen, G. (2019). Influence of the three-dimensional printing technique and printing layer thickness on model accuracy. *Journal of Orofacial Orthopedics*, *80*(4), 194–204. https://doi.org/10.1007/s00056-019-00180-y

Zmitrowicz, A. (2006). WEAR PATTERNS AND LAWS OF WEAR-A REVIEW. In *JOURNAL OF THEORETICAL AND APPLIED MECHANICS* (Vol. 44).

CURRICULUM VITAE (CV)

PERSONAL DATA:

Name and Surname: Abdurrahman GÜNGÖR

Education:

Master's Degree	Gaziantep University
2020-2023	Mechanical Engineering
	Construction and Manufacturing Department
Bachelor's Degree	Gaziantep University
2013-2020	Mechanical Engineering
High School	Bülent Ecevit Anatolian High School-Nicosia/Cyprus
2008-2012	

Experience:

2019/09-2019/12	Intern Engineer - Örnek Machine
2020/01-2020/07	Mechanical Engineer - Örnek Machine
2020/08-2021/02	Mechanical Engineer – Eruslu Tekstil SAN.VE TİC A.Ş
2021/06-	Mechanical Engineering – Orenda Yapı Denetim LTD.

International Conference

1) Failure Analysis of 3D- Printed and Conventionally Manufactured Polymer Gears, The 3rd International Conference of Materials and Engineering Technology (TICMET 2021).**117-126**, 05/11/2021-06/11/2021